Highlights of experimental results on heavy-ion physics from ALICE

LFC22: STRONG INTERACTIONS FROM QCD TO NEW STRONG DYNAMICS AT LHC AND FUTURE COLLIDERS

30 August 2022
ECT*, Strada delle Tabarelle 286, I-38123
Villazzano TRENTO (TN)

Alberto Calivà for the ALICE Collaboration
University of Salerno and INFN

UNIVERSITÀ DEGLI STUDI DI SALERNO

INFN Istituto Nazionale di Fisica Nucleare
SEZIONE DI NAPOLI
Gruppo Collegato di Salerno

CERN

ALICE

Outline

(Brief) introduction to heavy-ion physics and the ALICE experiment

Selected results on:

- Heavy quarkonia
- Open heavy flavor
- Jets
- Light flavor
- Direct photons and dileptons

Introduction

One of the goals of studying ultrarelativistic heavy-ion collisions:
> characterize phase diagram of QCD matter

https://cds.cern.ch/record/2025215

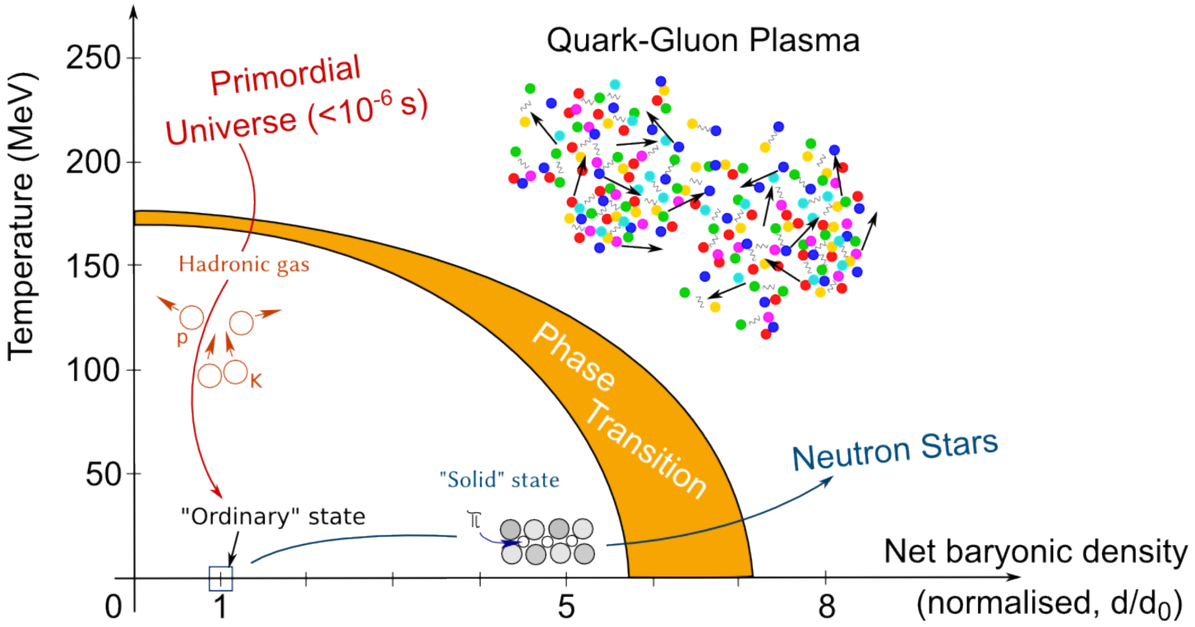

A. Bazavov *et al.* (HotQCD Collaboration)
Phys. Rev. D 90 (2014) 094503

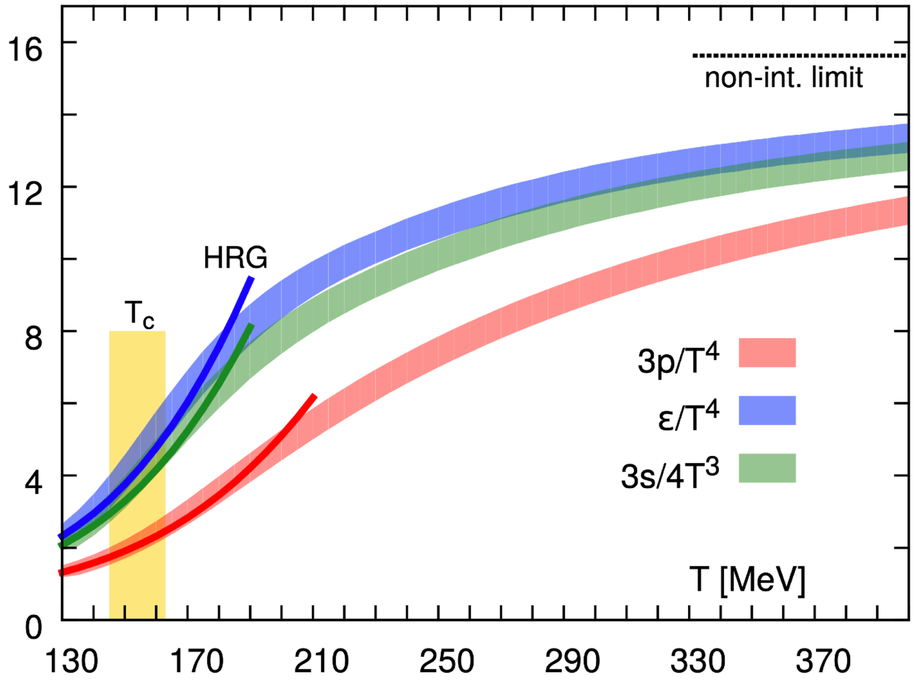

Quark-gluon plasma: deconfined phase of quarks and gluons

Phase transition at LHC is a smooth crossover → similar to early universe (~few μs after the Big Bang)

Time evolution of HI collisions

Time evolution of ultrarelativistic heavy-ion collisions:

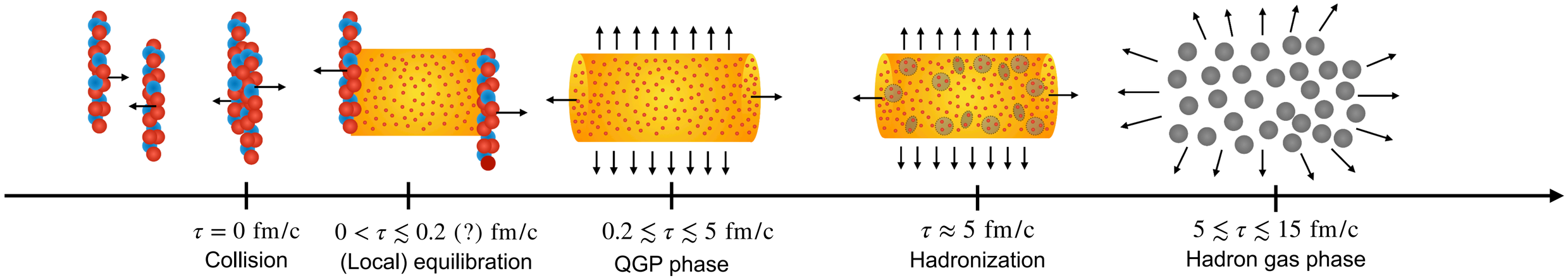

Different probes carry complementary information on different stages of the collision

Characterization of QGP and hadron gas properties from overall picture

Summary of experimental highlights from ALICE will be published in a review paper that is in internal review

Chemical freezeout ($T_{chem} \approx 155$ MeV):
- inelastic interactions cease
- hadron abundances fixed

Kinetic freezeout ($T_{kin} \approx 100$ MeV):
- Momentum spectra "frozen"

The ALICE experiment

Inner Tracking System (ITS)
- 6 layers of silicon detectors
- Tracking and particle identification at low momentum
- Primary and secondary vertex

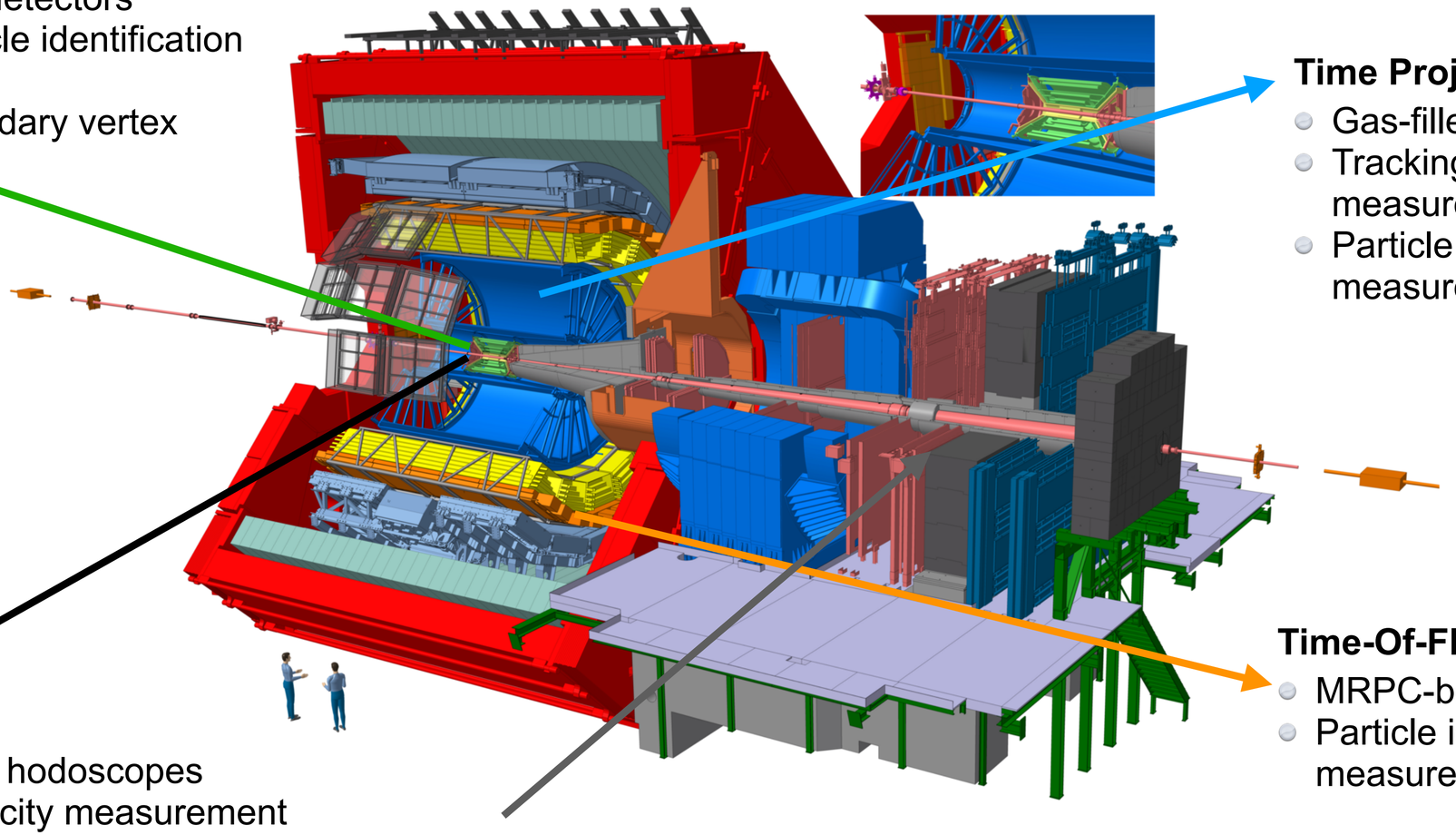

Time Projection Chamber (TPC)
- Gas-filled tracking detector
- Tracking and momentum measurement
- Particle identification via d*E*/d*x* measurement

V0 detectors
- Forward scintillator hodoscopes
- Trigger and multiplicity measurement

Time-Of-Flight detector (TOF)
- MRPC-based timing detector
- Particle identification via time-of-flight measurement

Muon Spectrometer
- Absorber and tracking stations for muons

Geometry of the collision

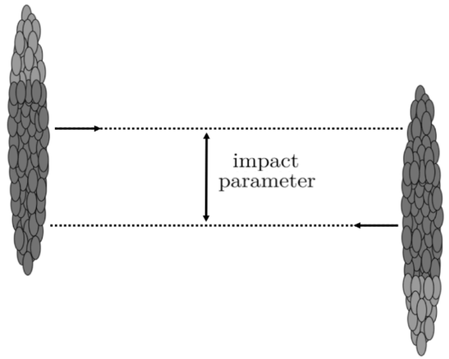

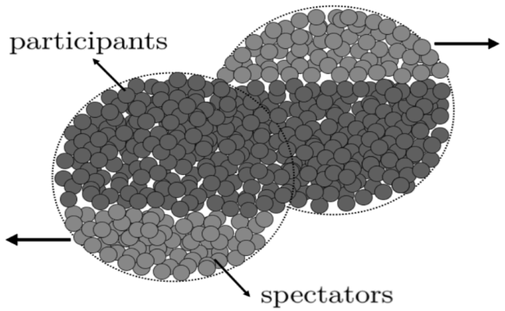

Int. J. Mod. Phys. A29, 1430044 (2014)

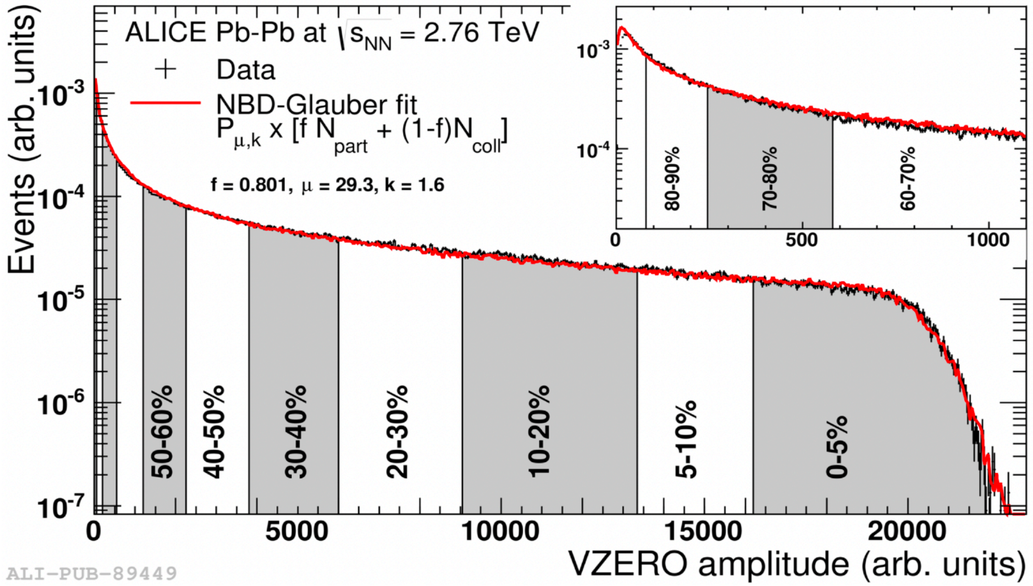

Centrality related to impact parameter *b*:

$$0 < b < 2R$$

Most central collisions

Most peripheral collisions

Centrality classes defined experimentally by integrating the amplitude distribution measured by the V0 scintillators

$$c = \frac{1}{\sigma_{\text{tot}}} \int_{V_0}^{\infty} \frac{d\sigma}{dV} dV$$

Symmetry plane and elliptic flow

Initial geometrical asymmetry of non-central collisions results in azimuthal asymmetry of particle emission:

$$\frac{dN}{d\phi} = \frac{N}{2\pi}\left[1 + 2\sum_{n=1}^{\infty} v_n \cos(n(\phi - \Psi_n))\right]$$

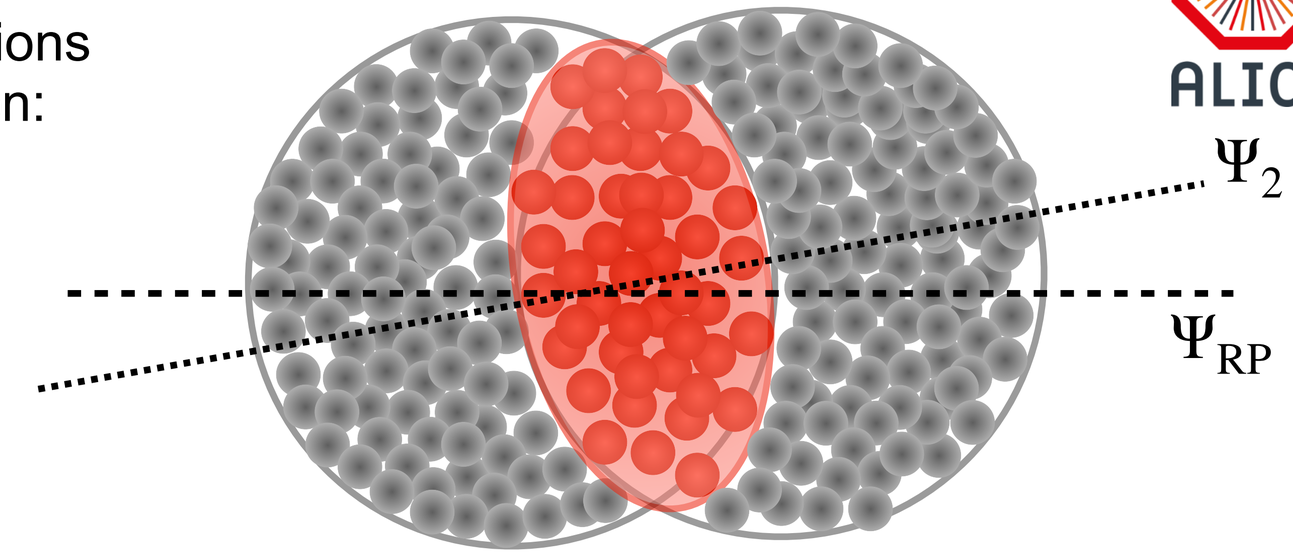

The second harmonic is the **elliptic flow**

$$v_2 = < \cos(2(\phi - \Psi_2)) >$$

connected to initial state eccentricity

$$\epsilon = < \frac{x^2 - y^2}{x^2 + y^2} >$$

Stronger pressure gradient along symmetry plane

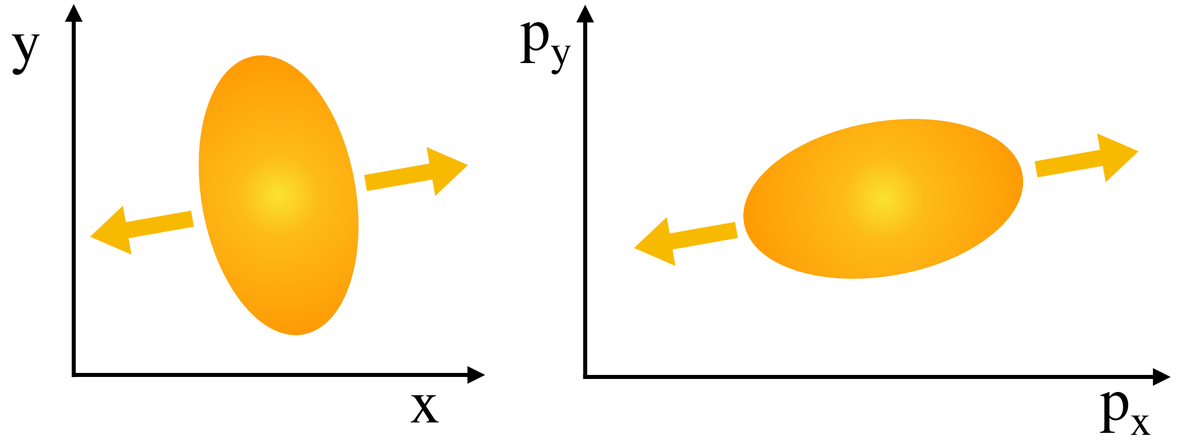

Heavy Quarkonia

J/ψ R_{AA}: RHIC vs. LHC

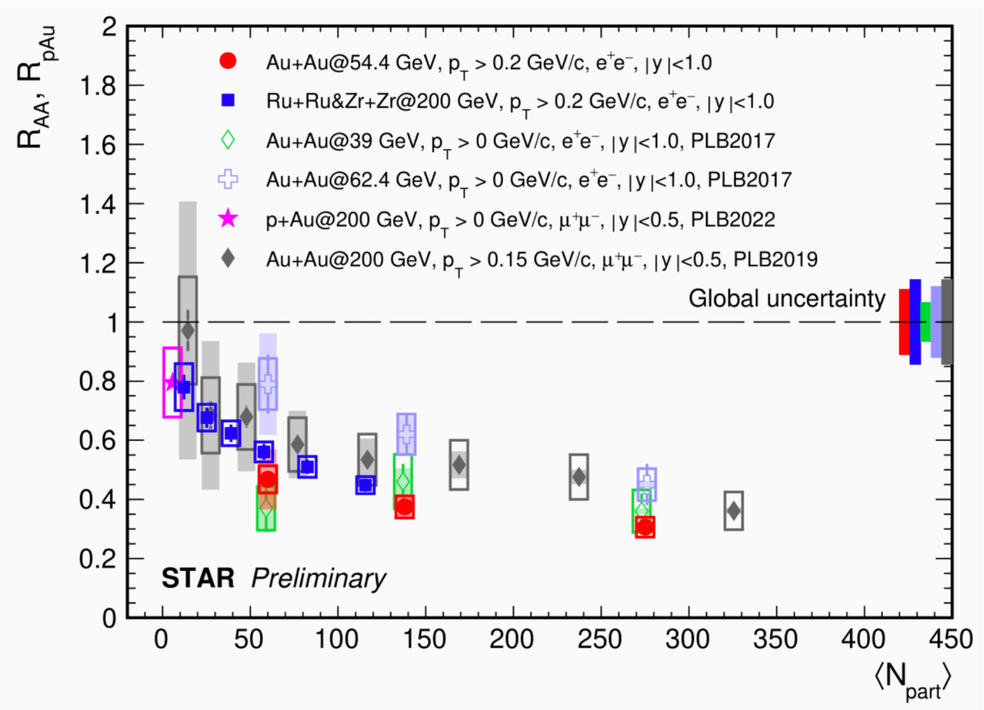

Nuclear modification factor R_{AA}

$$R_{AA,pA} = \frac{1}{\langle N_{coll} \rangle} \frac{\text{Yield (pA, AA)}}{\text{Yield (pp)}}$$

R_{AA} of inclusive J/ψ at midrapidity decreases with $\langle N_{part} \rangle$ at RHIC energies

J/ψ R_{AA}: RHIC vs. LHC

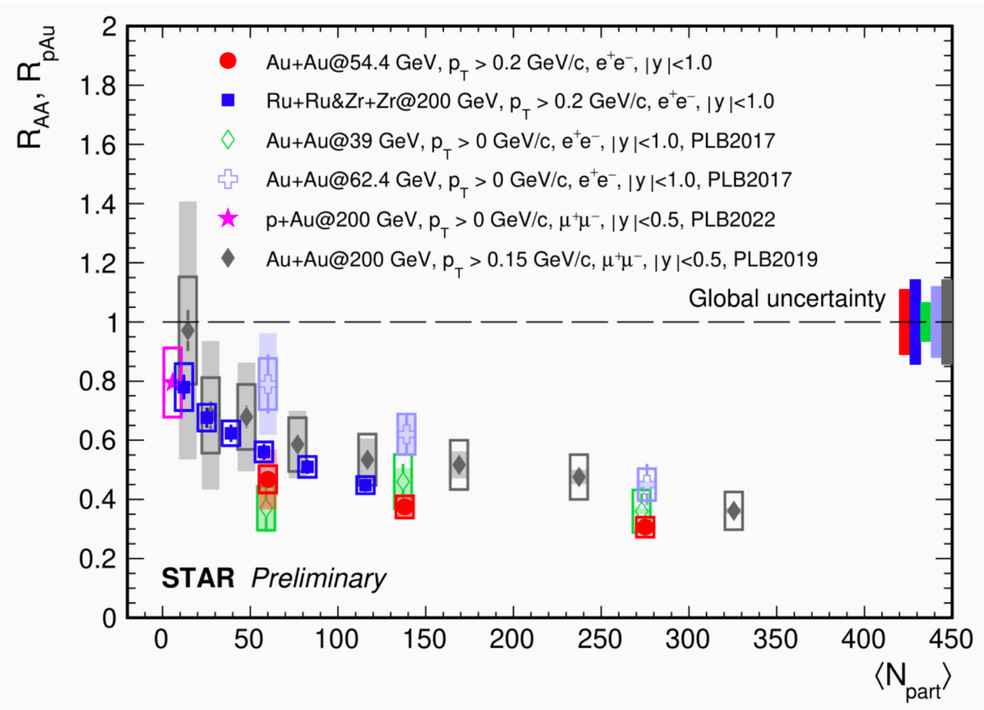

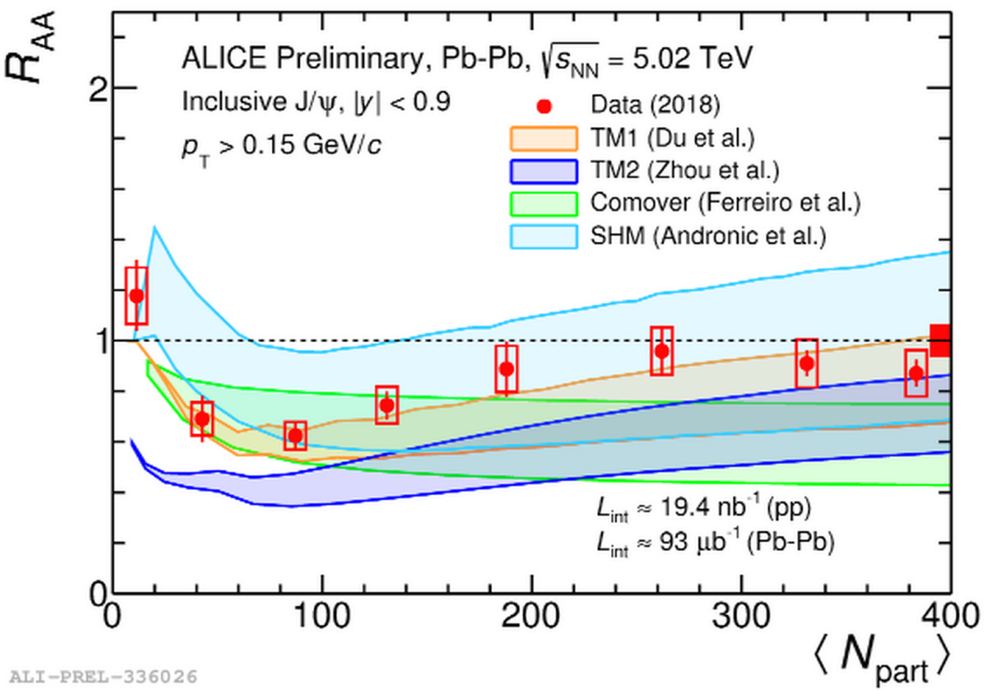

Nuclear modification factor R_{AA}

$$R_{AA,pA} = \frac{1}{\langle N_{coll} \rangle} \frac{\text{Yield (pA, AA)}}{\text{Yield (pp)}}$$

R_{AA} of inclusive J/ψ at midrapidity decreases with $\langle N_{part} \rangle$ at RHIC energies

At LHC energy: in central Pb-Pb collisions ~ 1 $c\bar{c}$ pair per fm^3 enhancemnt of the J/ψ R_{AA} with $\langle N_{part} \rangle$ → sign of $c\bar{c}$ recombination

Svetitsky PRD 37 (1988) 2484, PBM & Stachel PLB 490 (2000) 196,
Thews et al PRC 63 (2001) C549005, Andronic et al, PLB 652 (2007) 259

J/ψ R_{AA} vs. p_T

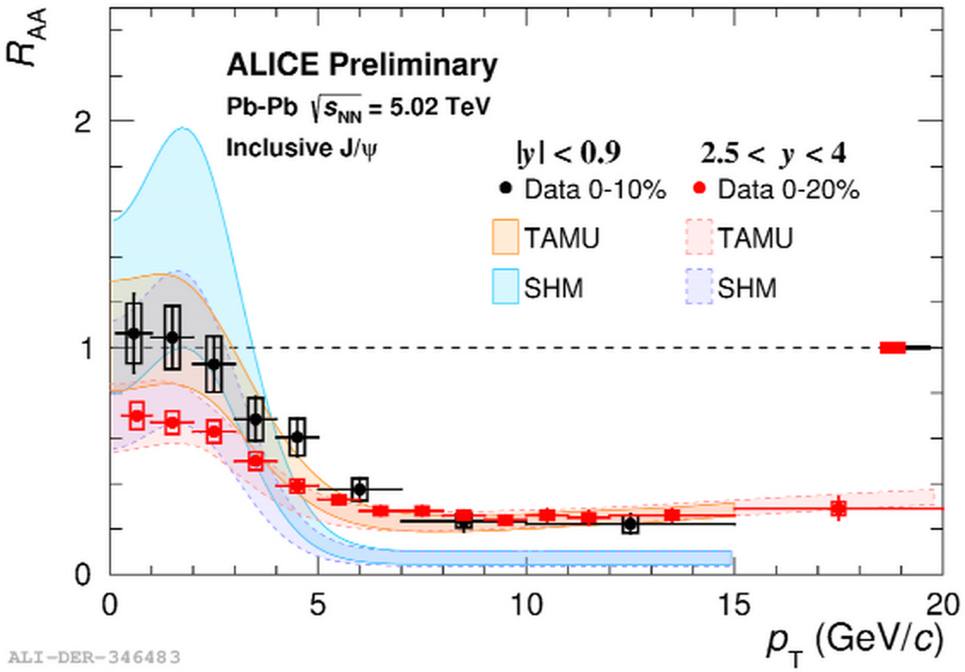

R_{AA} of inclusive J/ψ:

- Rise at low p_T (stronger effect at midrapidity): **decisive signature of recombination**
- Models that include (re)generation (SHMc and TAMU) describe the data at low p_T

J/ψ R_{AA} vs. p_T

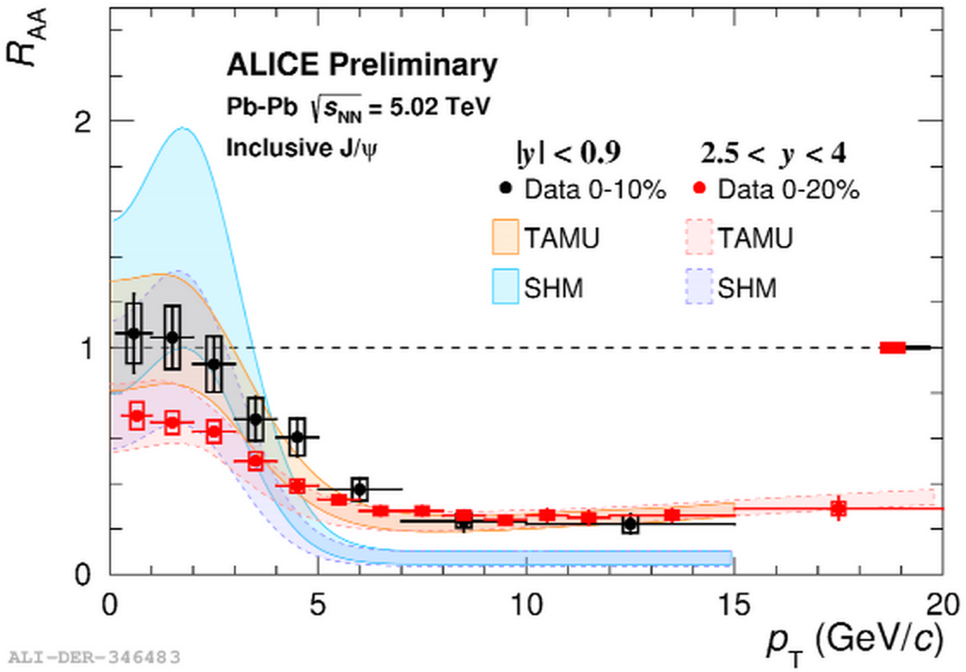

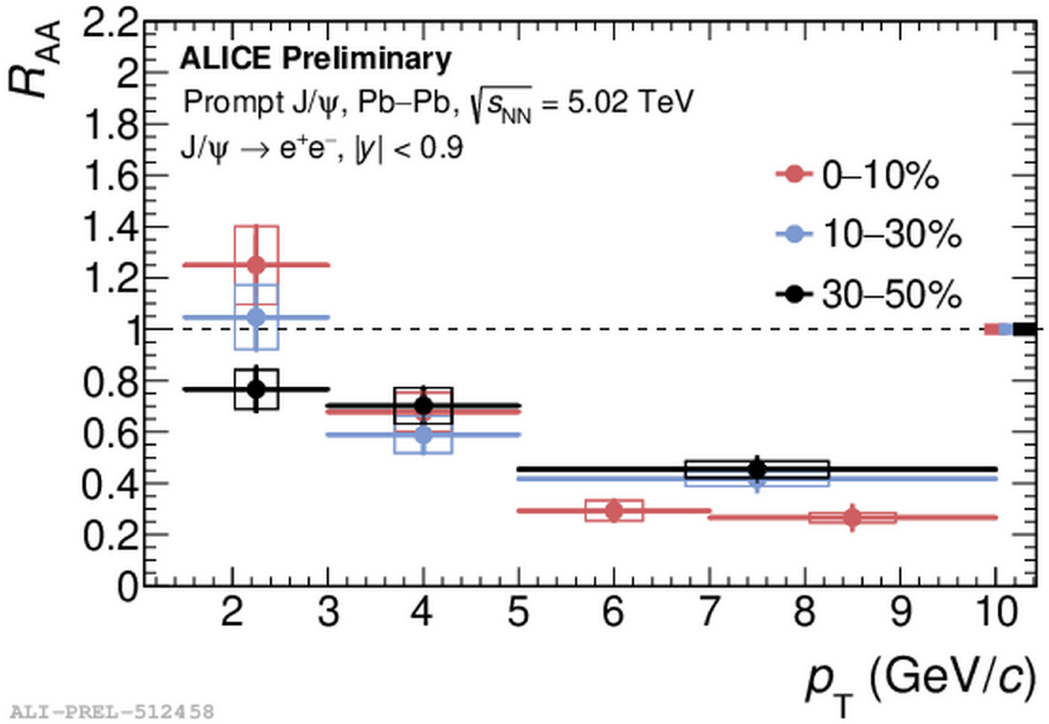

R_{AA} of inclusive J/ψ:

- Rise at low p_T (stronger effect at midrapidity): **decisive signature of recombination**
- Models that include (re)generation (SHMc and TAMU) describe the data at low p_T

Rise of R_{AA} at low p_T as an effect of recombination confirmed by prompt J/ψ (c→J/ψ)
> clear centrality dependence

TAMU: M. He et al., PLB 735 (2014) 445, SHMc: A. Andronic et al., PLB 571 (2003) 36

Sequential suppression of charmonia

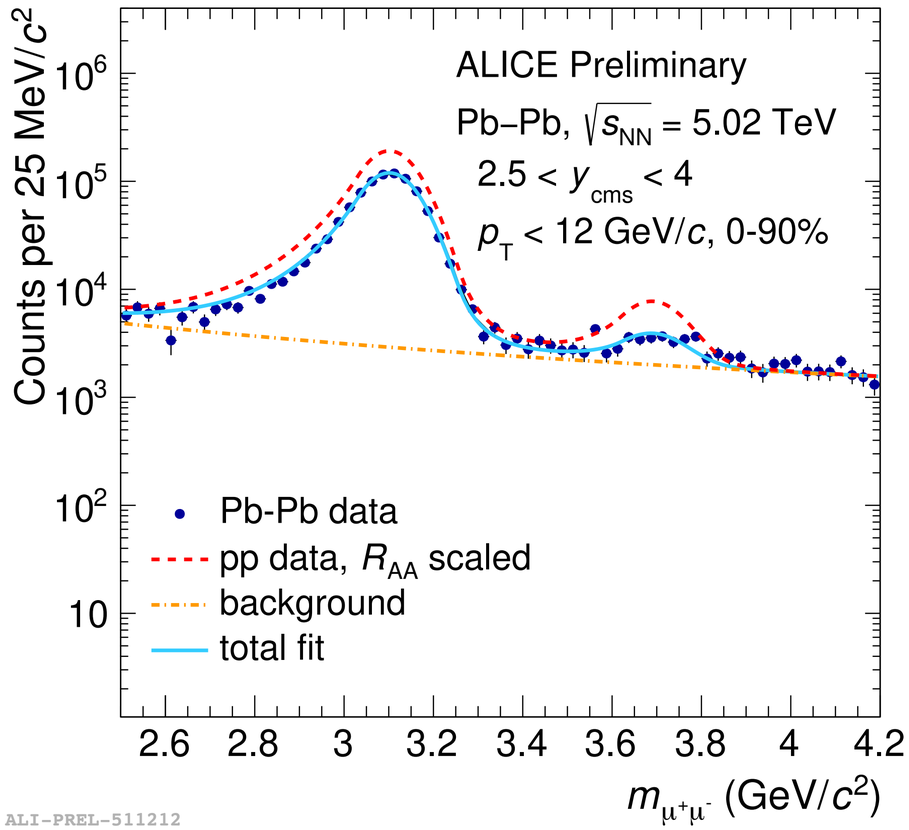

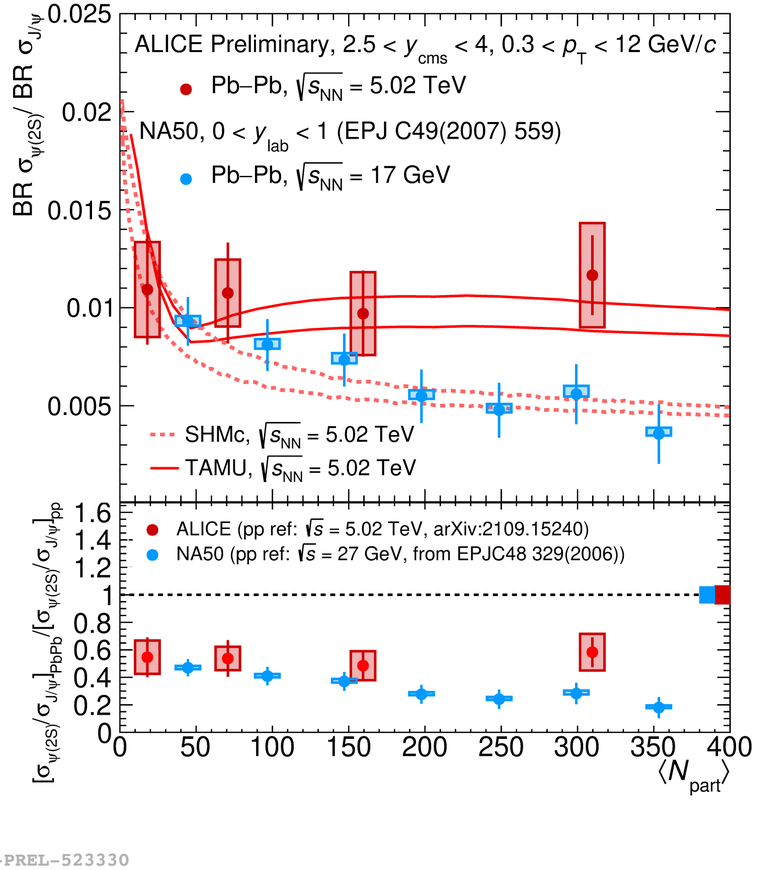

Stronger suppression of ψ(2S) wrt J/ψ
> sequential suppression of charmonia?

Centrality dependence of ψ(2S)/J/ψ described by TAMU and slightly underestimated by SHMc

(Re)generation of charmonia

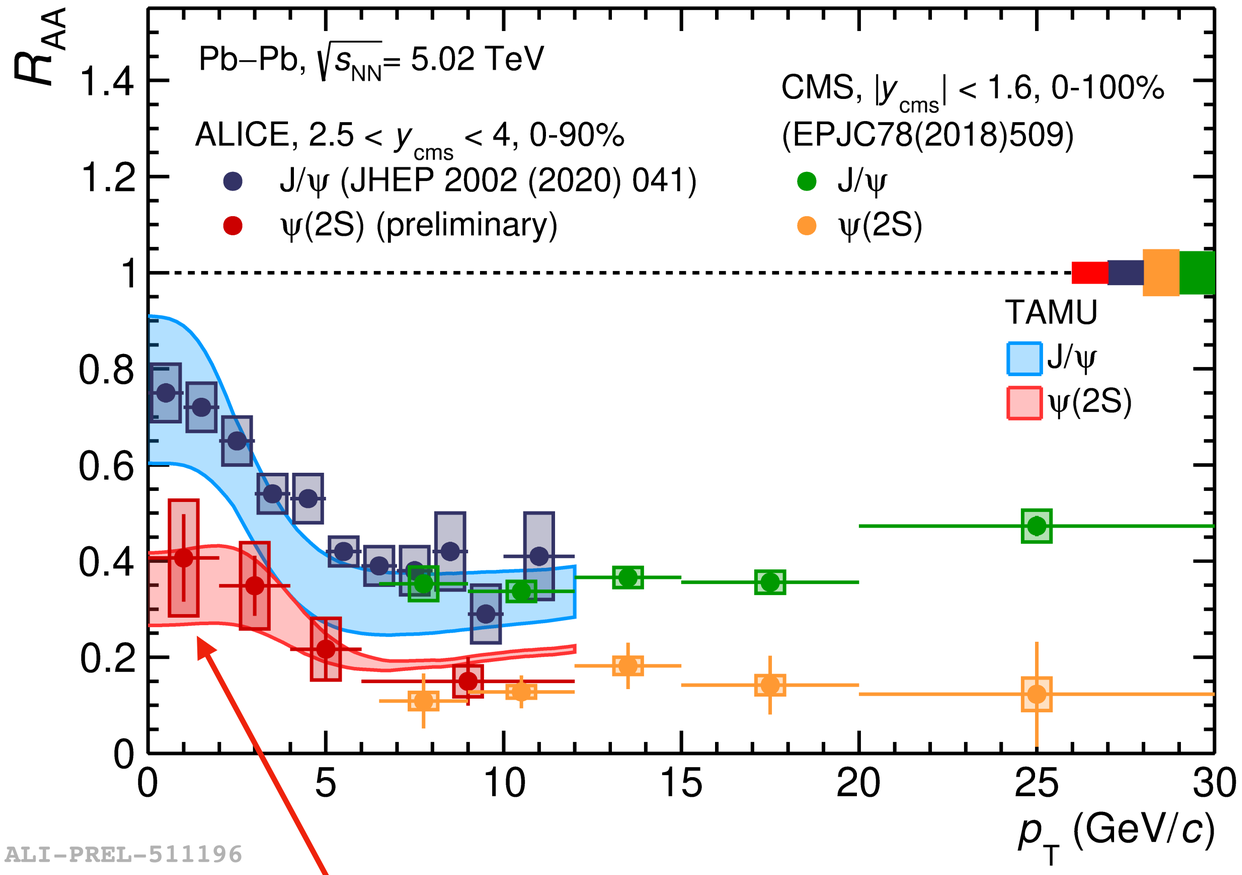

ψ(2S) measurement extended to p_T = 0

R_{AA} of ψ(2S) increases going to lower p_T
> qualitatively similar to J/ψ
→ ψ(2S) production via $c\bar{c}$ recombination?

- p_T dependence of R_{AA} reproduced by TAMU

  X. Du and R. Rapp, Nucl. Phys. A943 (2015)

Open Heavy Flavor

Non-prompt J/ψ and D mesons

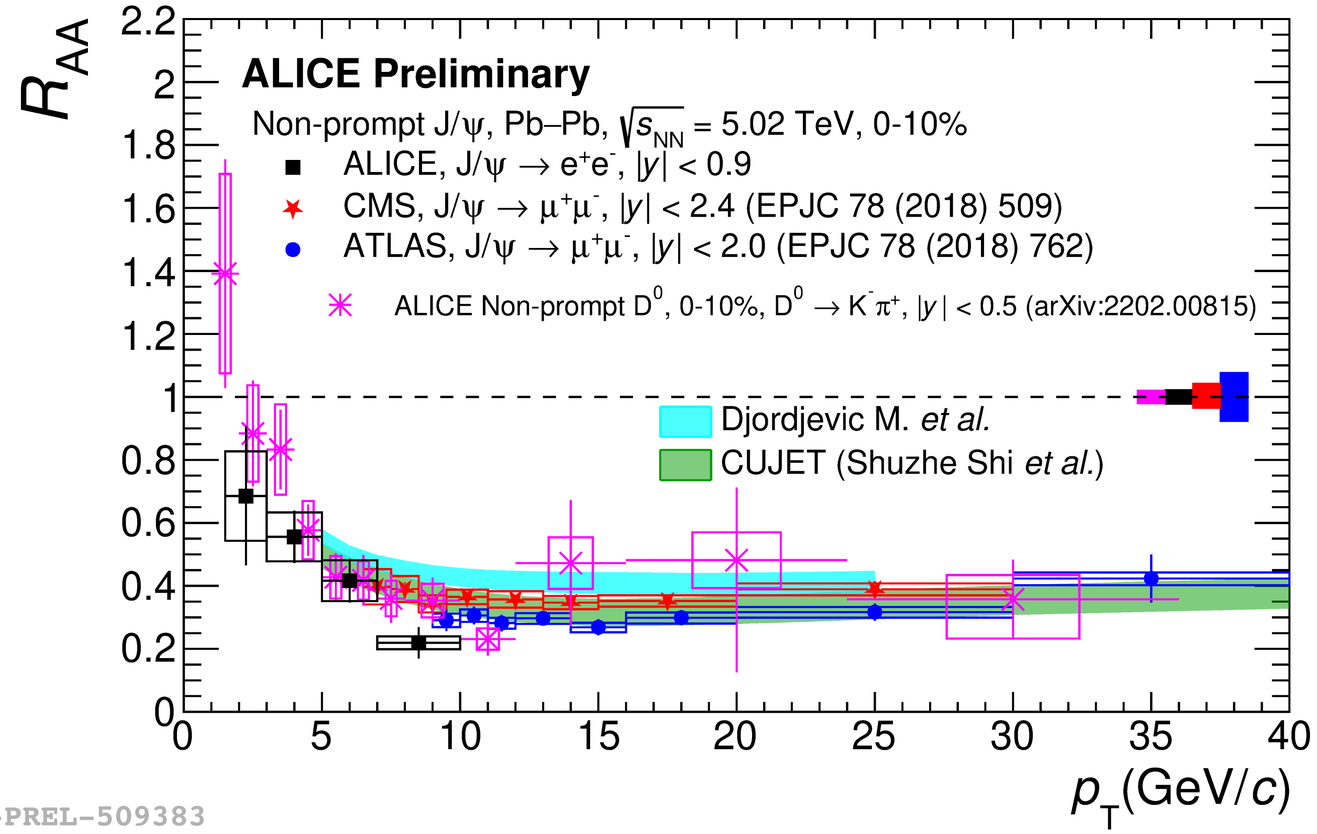

Non-prompt D^0: b→c→D^0

Non-prompt J/ψ: b→c→J/ψ

R_{AA} of hadrons containing b quark via measurements of non-prompt J/ψ and D mesons

Unprecedented access to low p_T region

R_{AA} of prompt and non-prompt D^0

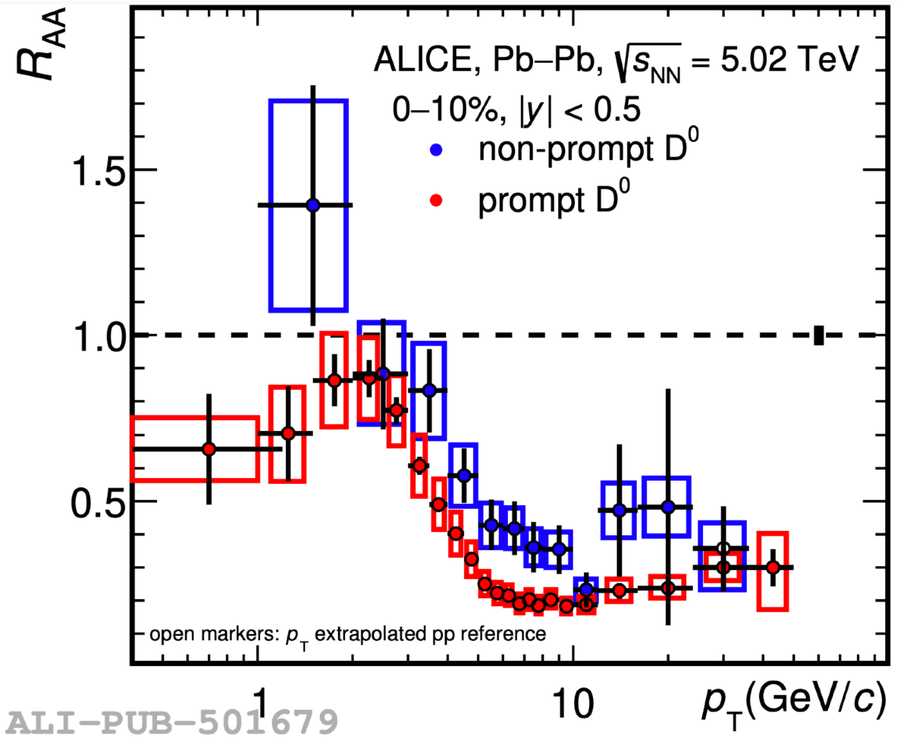

ALI-PUB-501679

Prompt D^0: c→D^0

Non-prompt D^0: b→c→D^0

arXiv:2202.00815 [nucl-ex]

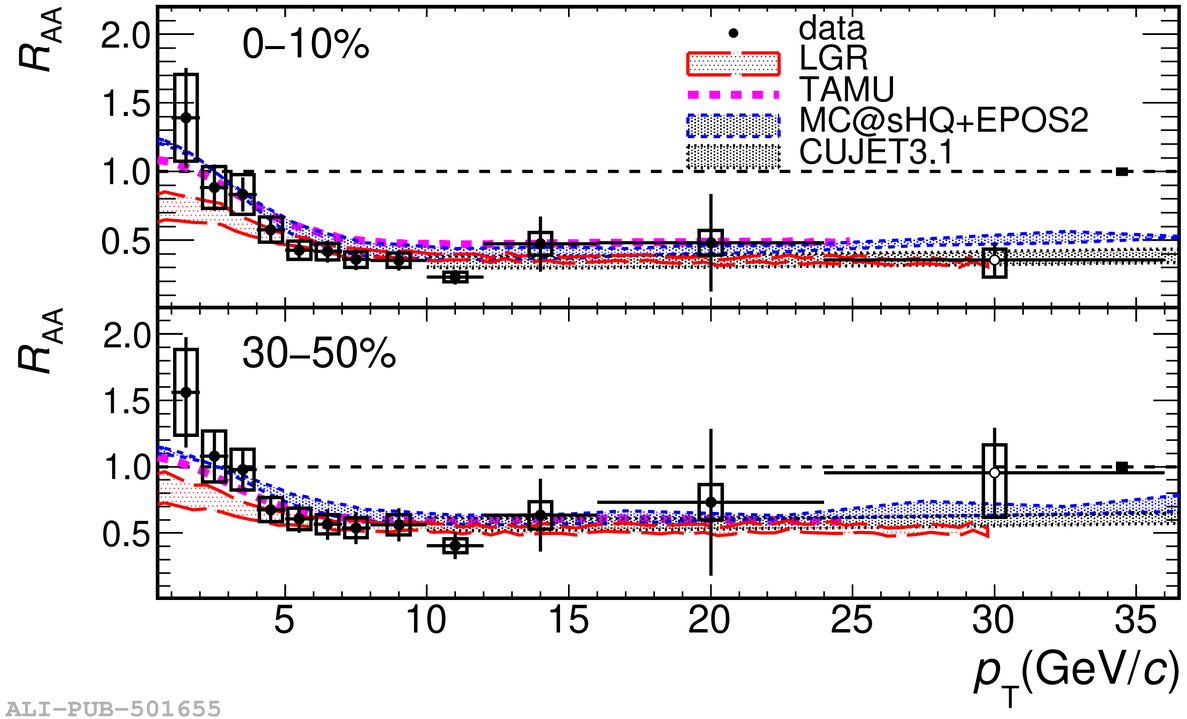

ALI-PUB-501655

Bottom shows less suppression than charm

Theoretical models that include collisional and radiative energy loss describe the data within uncertainties

Interaction with medium

arXiv:2202.00815 [nucl-ex]

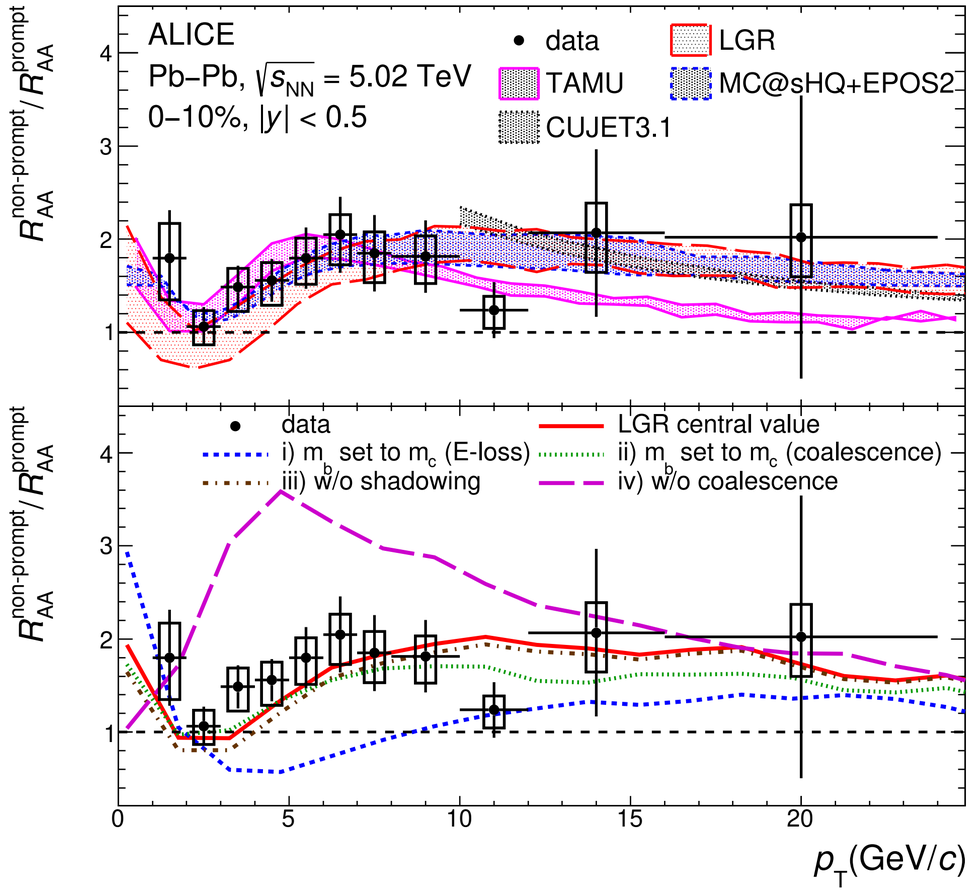

ALI-PUB-501659

R_{AA} (b) / R_{AA} (c) is sensitive to effects that are different for charm and bottom:

shadowing, interaction with medium, mass-dependent radiative energy loss, …

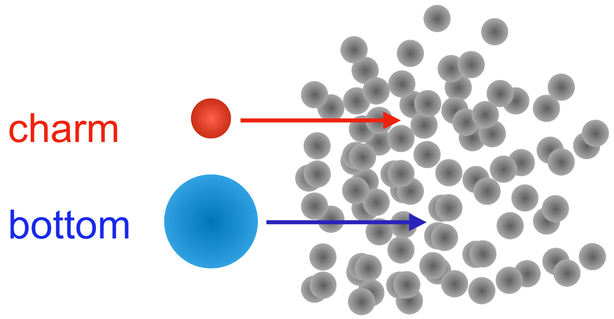

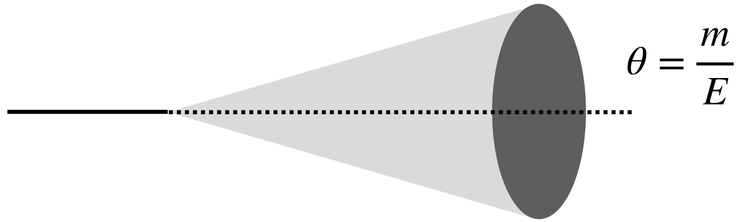

radiation suppressed inside a cone with aperture $\theta = m/E$ (dead cone)

The "valley" structure at low p_T is mainly due to formation of prompt D-mesons via quark coalescence

LGR: EPJC 80 (2020) 651, EPJC 80 (2020) 1113

R_{AA} and v_2 of prompt D-mesons

Prompt D^0, D^+, D^{*+}

JHEP 01 (2022) 174

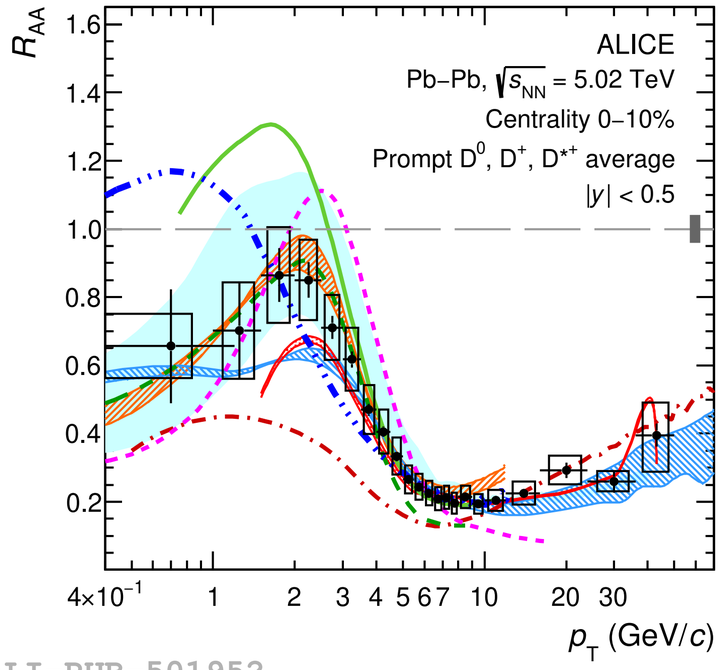

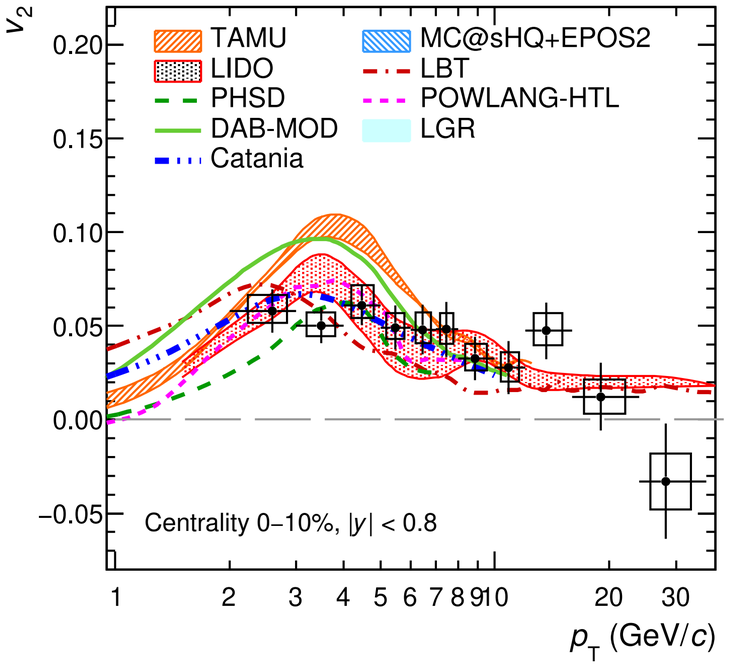

ALI-PUB-501952

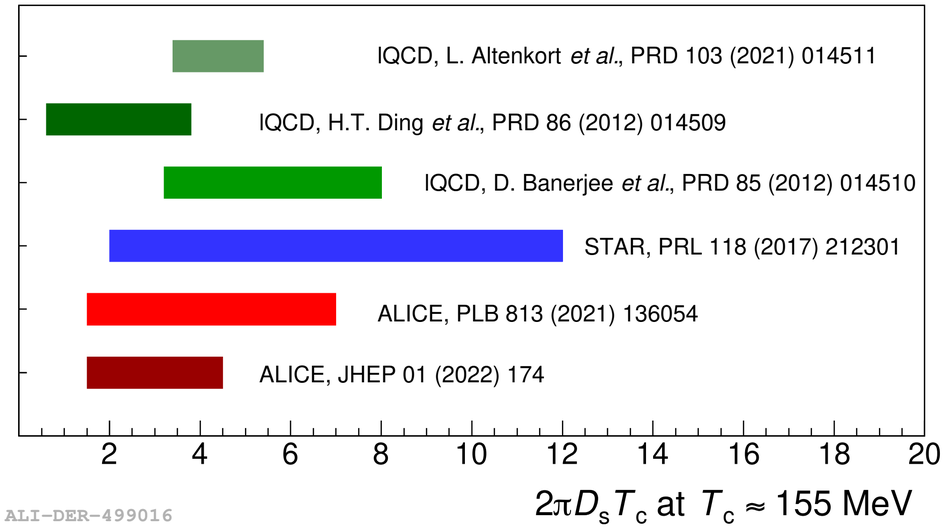

ALI-DER-499016

Most of the transport models describe both R_{AA} and v_2

> constraint on spatial diffusion coefficients

R_{AA} and v_2 of prompt D-mesons

Prompt D^0, D^+, D^{*+}

JHEP 01 (2022) 174

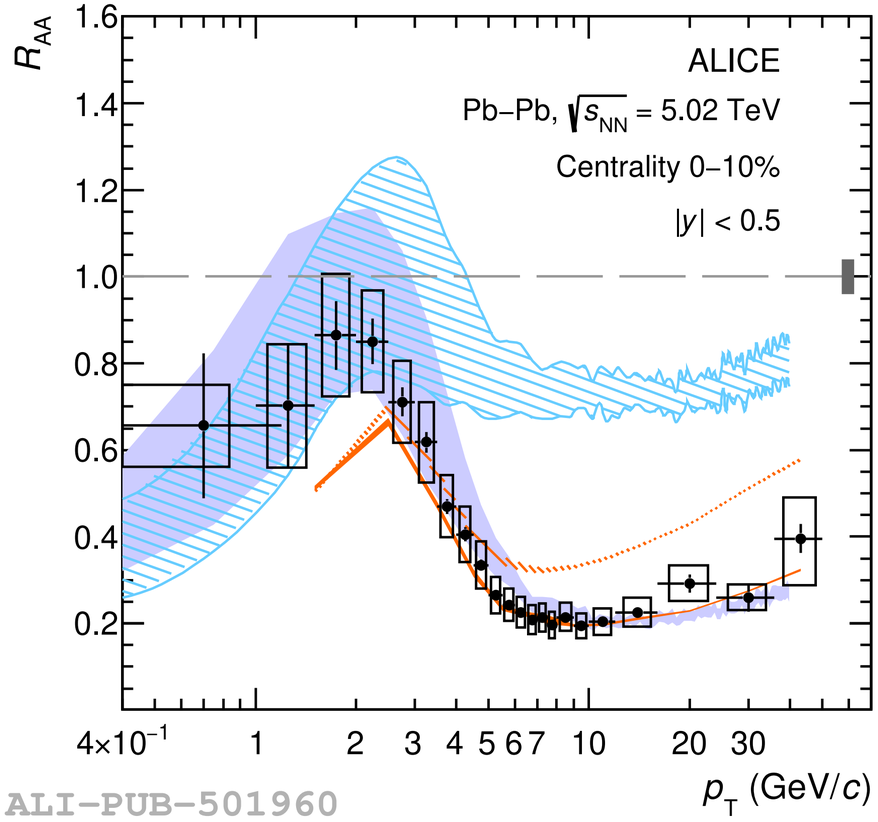

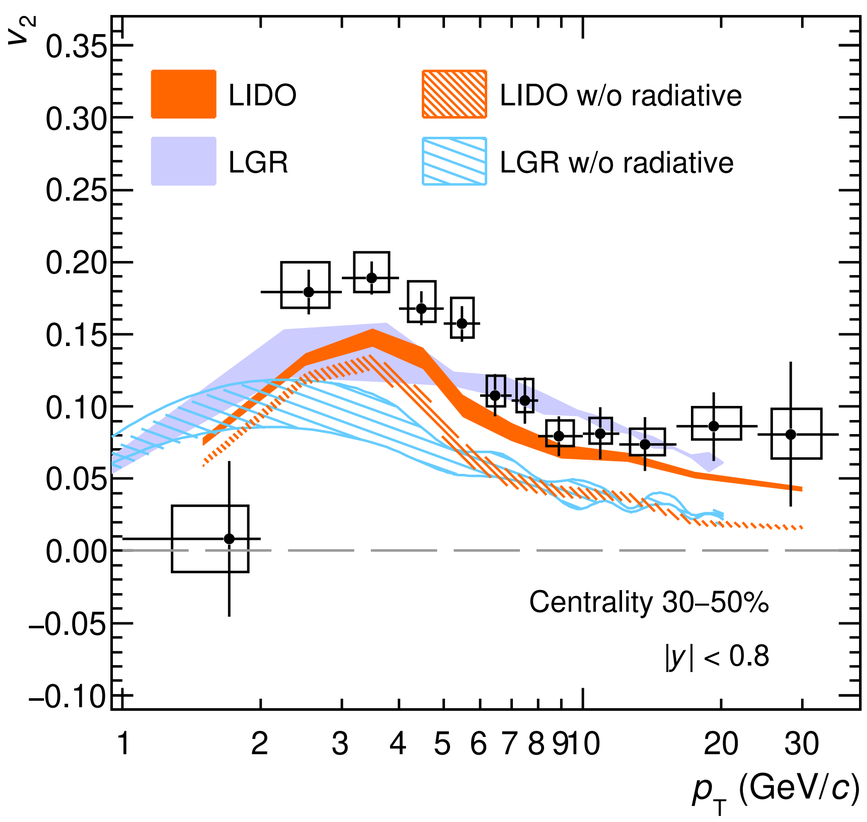

Radiative energy loss important to describe intermediate and high p_T

> small impact on low p_T region

Jets

Heavy-flavor vs. inclusive jets

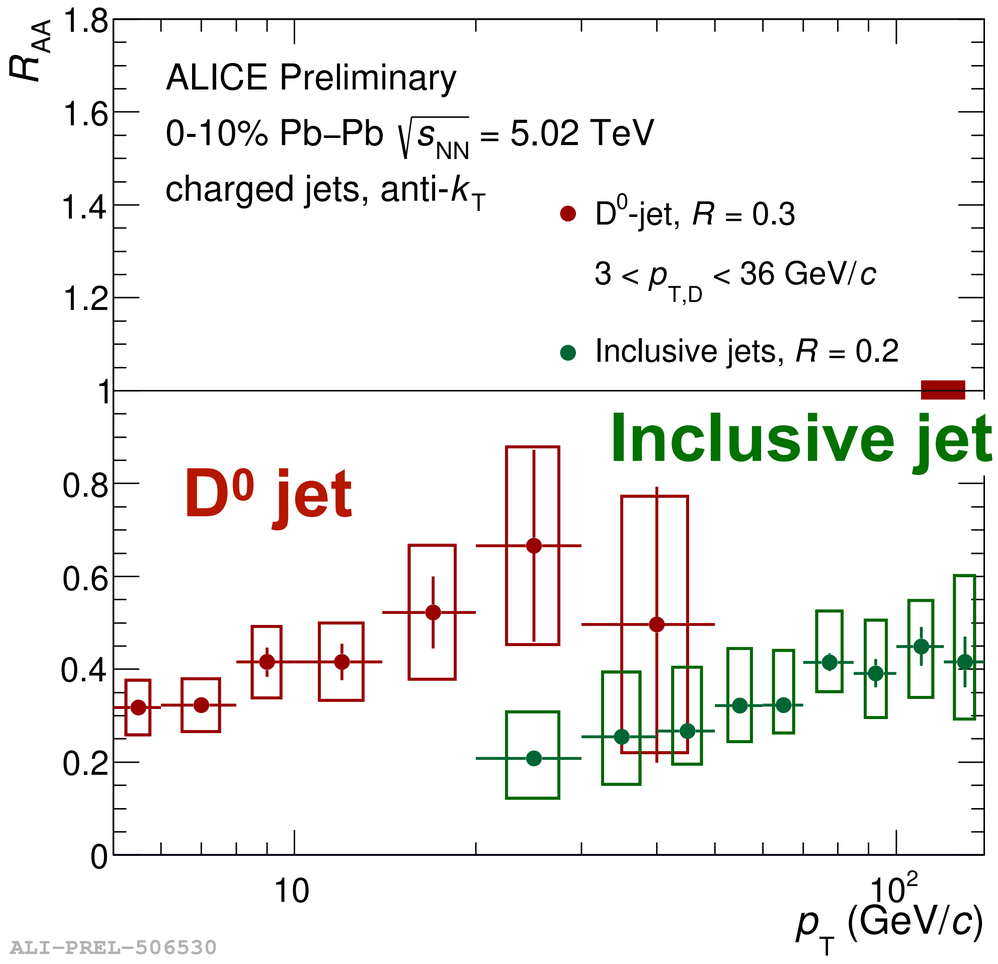

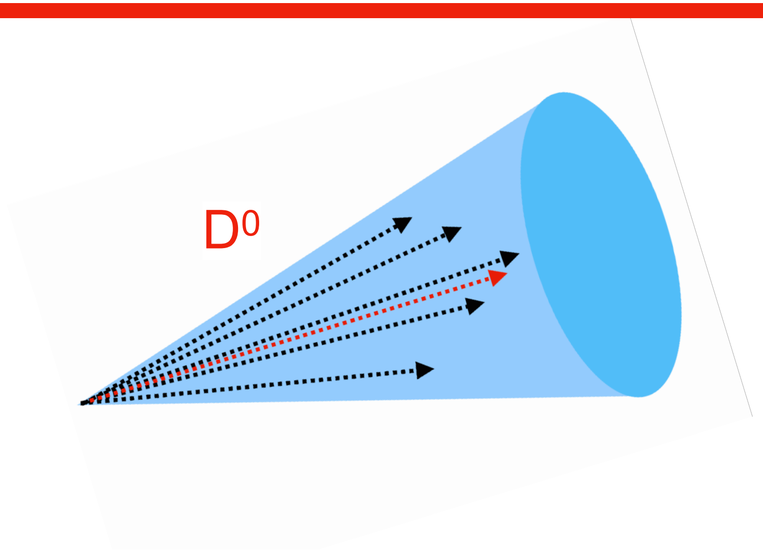

Hint of a higher R_{AA} of D^0-jets compared to inclusive jets in Pb-Pb collisions

Difference between quark and gluon energy loss and mass-dependent effects (dead cone)

Medium-induced jet modifications

Medium-induced jet modifications
studied using the jet grooming technique:
> find first hard splitting

Jet core more collimated in Pb-Pb wrt pp collisions

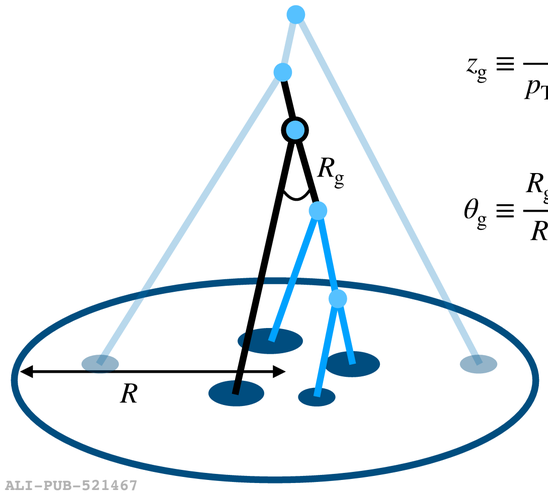

ALI-PUB-521467

$$z_g \equiv \frac{p_{T,\text{subleading}}}{p_{T,\text{leading}} + p_{T,\text{subleading}}}$$

$$\theta_g \equiv \frac{R_g}{R} \equiv \frac{\sqrt{\Delta y^2 + \Delta\varphi^2}}{R}$$

PRL 128 (2022) 102001

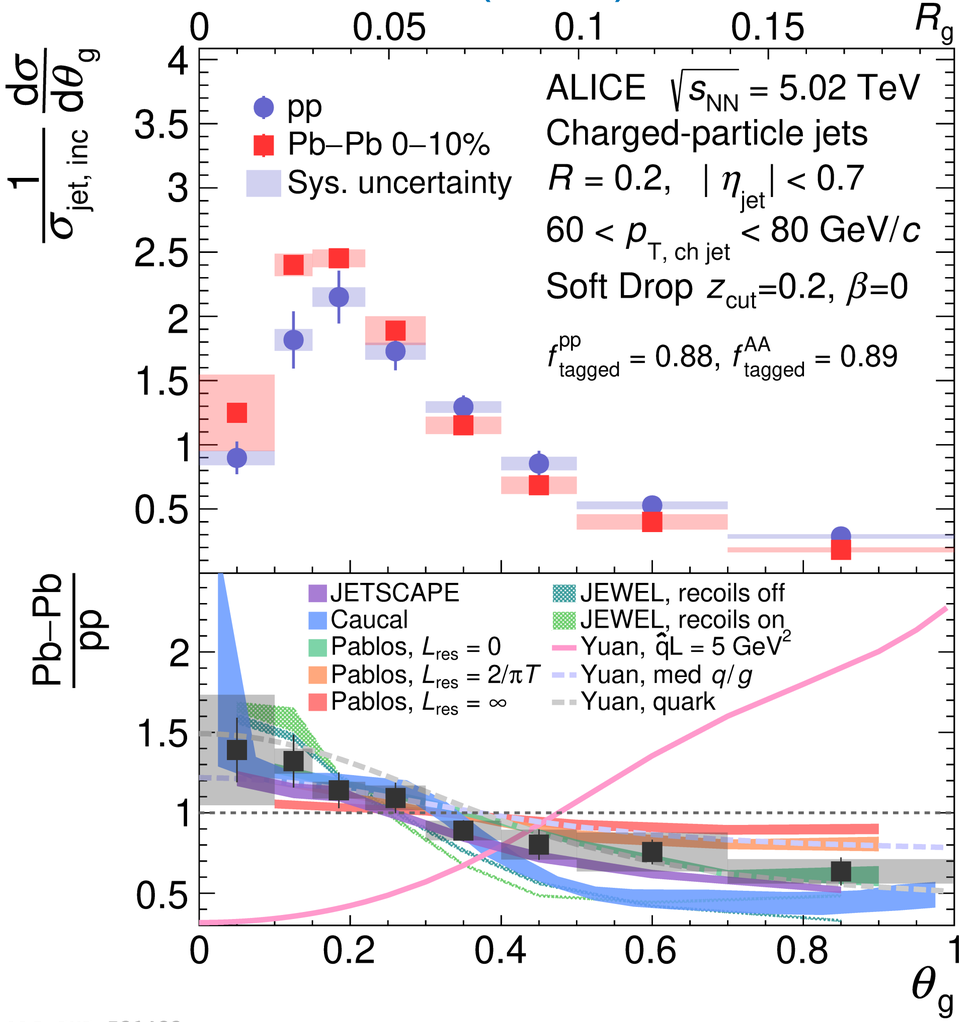

ALI-PUB-521482

Suppression of wider jets

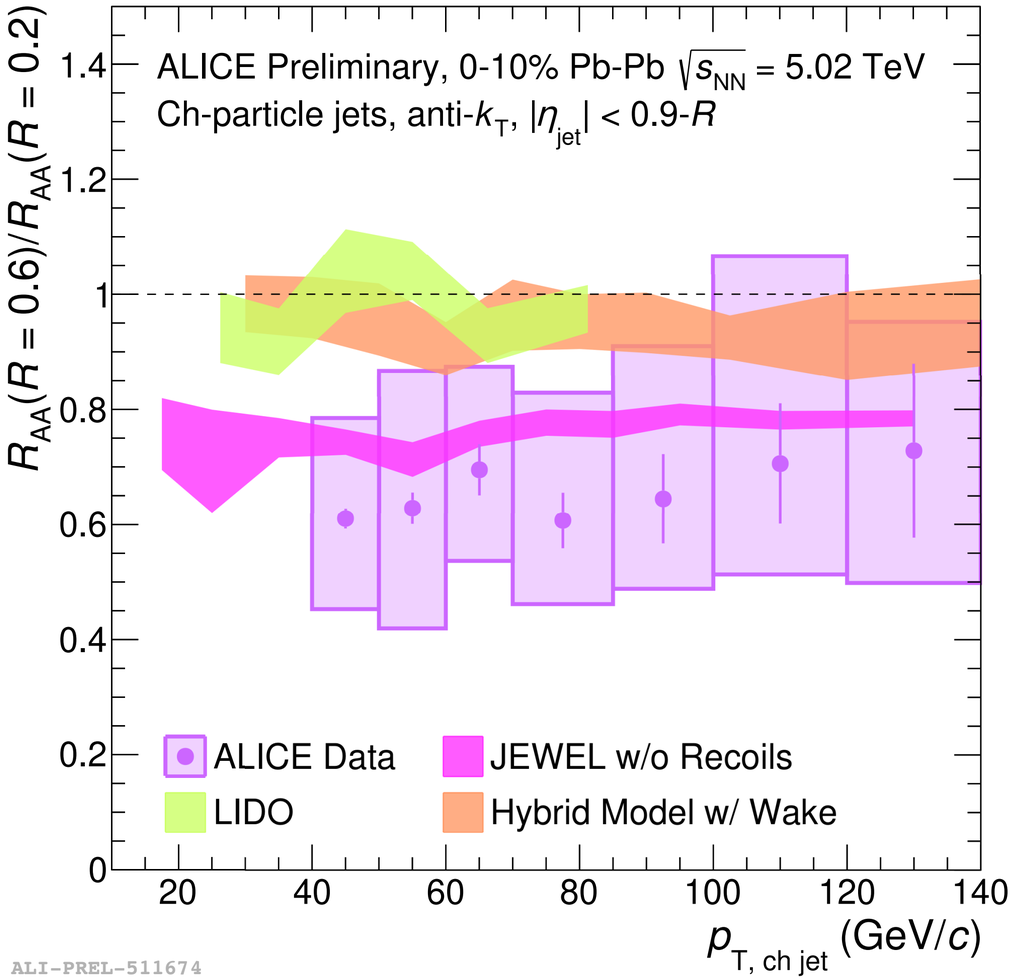

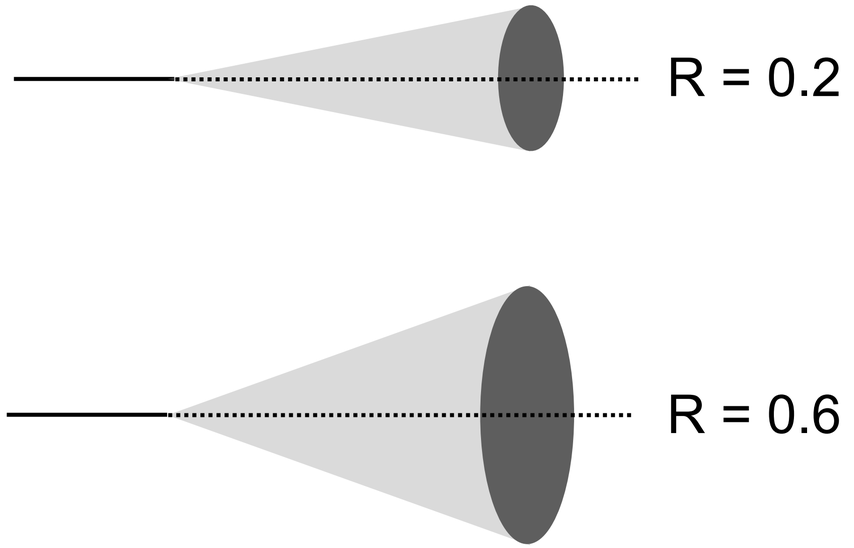

R-dependent suppression of jets in Pb-Pb collisions:

> wider jets are more suppressed wrt more collimated jets

Recoil jet in pp and Pb-Pb

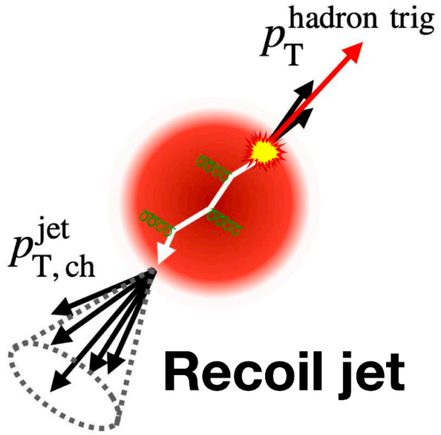

$$I_{\mathrm{AA}} = \frac{\Delta_{\mathrm{recoil}}(\mathrm{Pb-Pb})}{\Delta_{\mathrm{recoil}}(\mathrm{pp})}$$

Δ_{recoil} obtained from data-driven subtraction of uncorrelated background (including multi-parton interactions)

- hint of energy recovery at low jet momenta (with azimuthal broadening)
- data well described by JETSCAPE

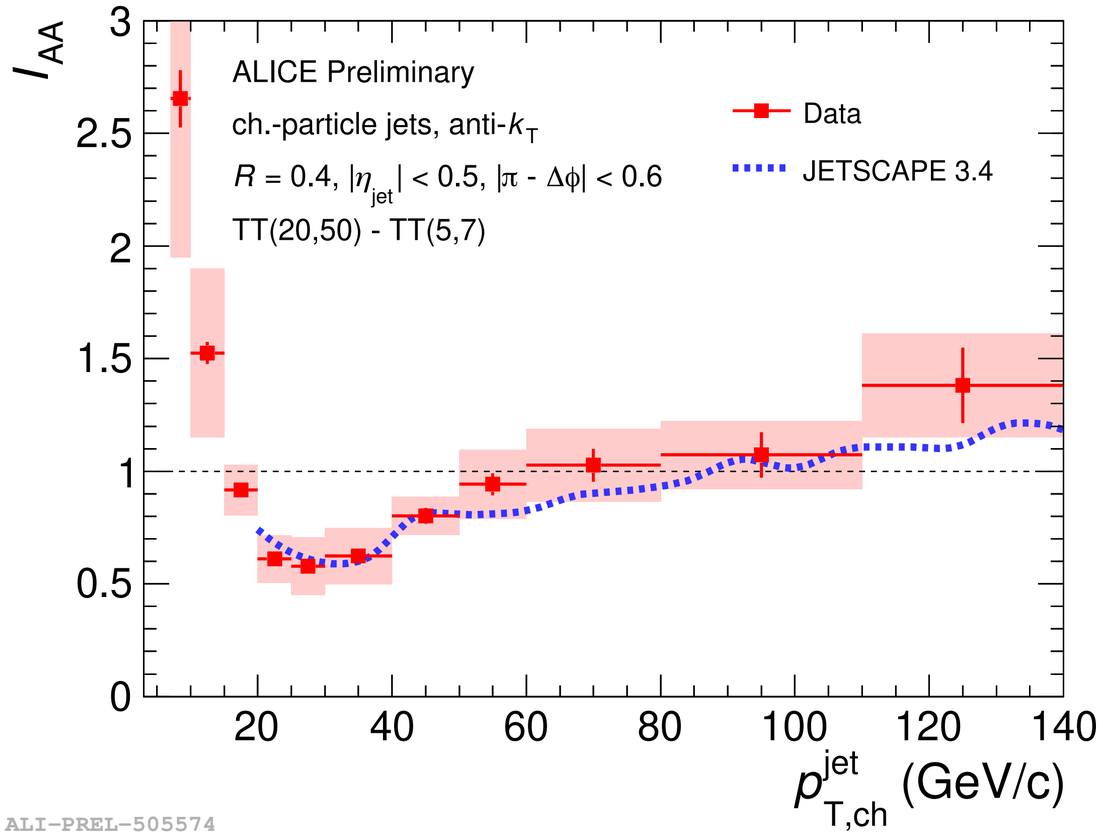

JETSCAPE: J. Putschke et al., arXiv:1903.07706 [nucl-th]

Light Flavor

Deuteron number fluctuations

arXiv:2204.10166 [nucl-ex]

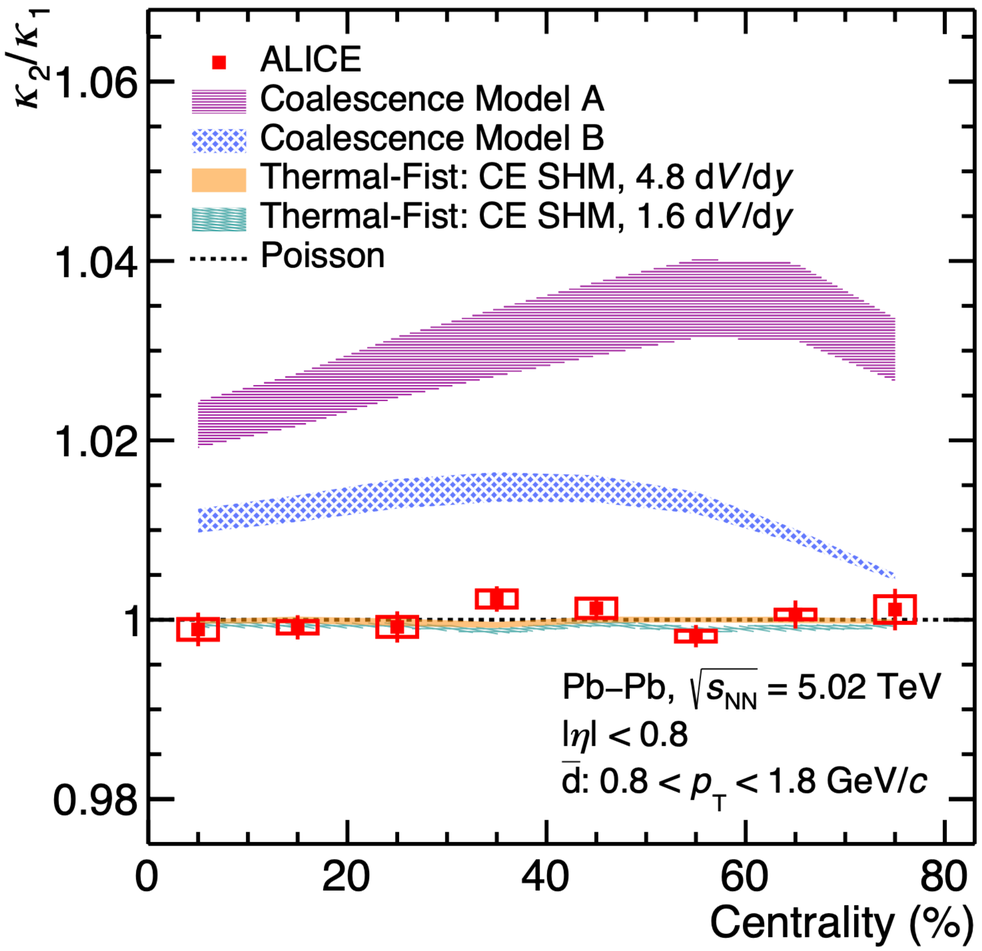

New observable based on event-by-event (anti)deuteron fluctuations to distinguish SHM and coalescence

$$\frac{\kappa_2}{\kappa_1} = \frac{\langle (n - \langle n \rangle)^2 \rangle}{\langle n \rangle}$$

Cumulant ratio favors canonical statistical model

Coalescence Model A: full correlation of *p* and *n*
Coalescence Model B: independent *p* and *n* fluctuations

Correlation volume

arXiv:2204.10166 [nucl-ex]

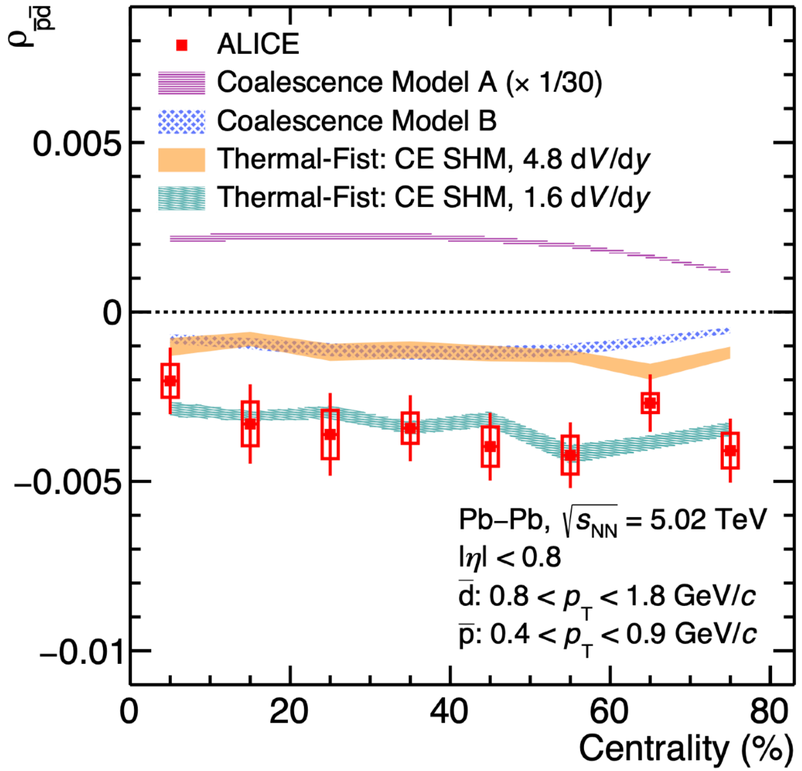

Pearson correlation $\rho_{\bar{p}\bar{d}}$ clearly indicates a correlation volume for baryon number conservation of 1.6 units of rapidity

Correlation volume

arXiv:2204.10166 [nucl-ex]

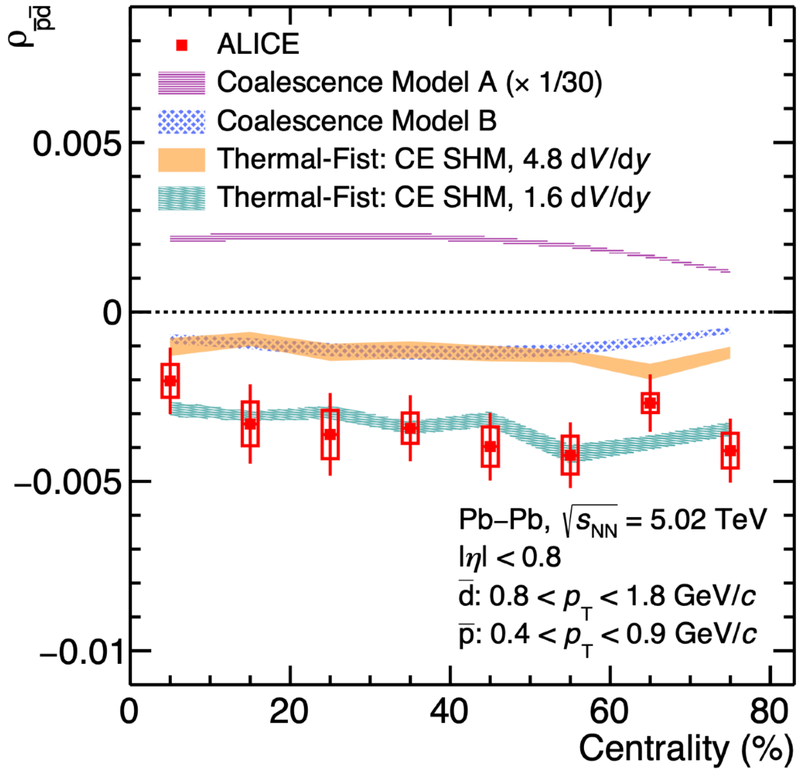

arXiv:2206.03343 [nucl-ex]

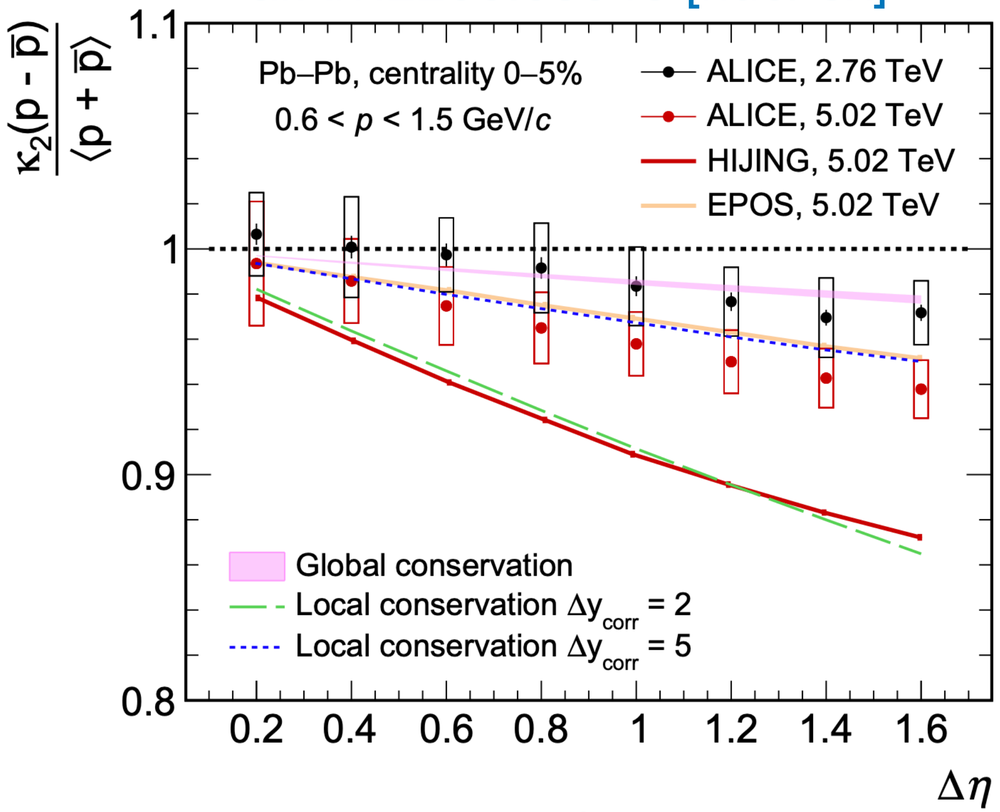

Pearson correlation $\rho_{\bar{p}\bar{d}}$ clearly indicates a correlation volume for baryon number conservation of 1.6 units of rapidity

> different from net-proton fluctuation results (Δy_{corr} = 5)

Precise μ_B measurement at LHC

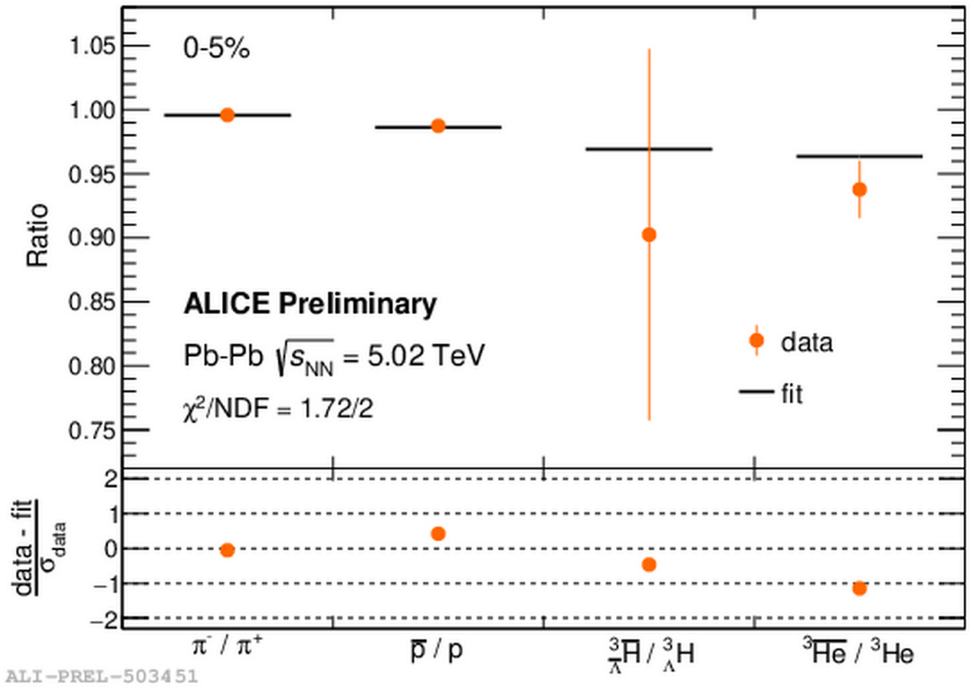

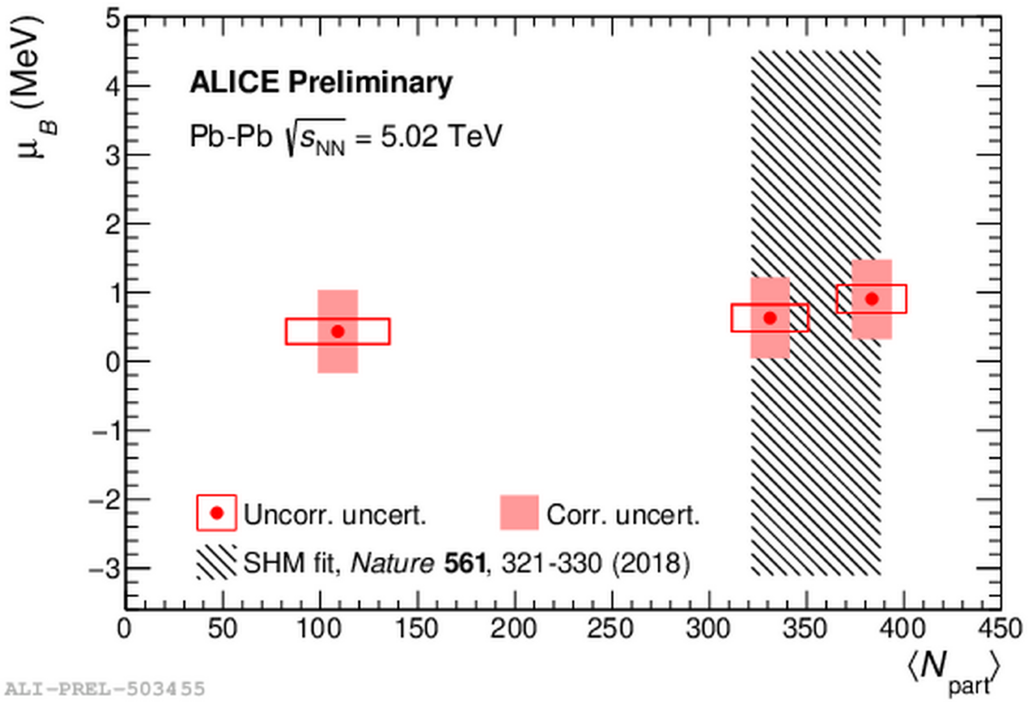

New measurement of antimatter/matter imbalance at the LHC

$$\bar{h}/h \propto \exp\left[-2\left(B + \frac{S}{3}\right)\frac{\mu_B}{T} - 2I_3\frac{\mu_{I_3}}{T}\right]$$

Uncertainties reduced wrt thermal model fit by one order of magnitude

> direct cancellation of correlated uncertainties in antimatter-to-matter ratios

${}^{3}_{\Lambda}\mathrm{H}$ Lifetime and B_{Λ}

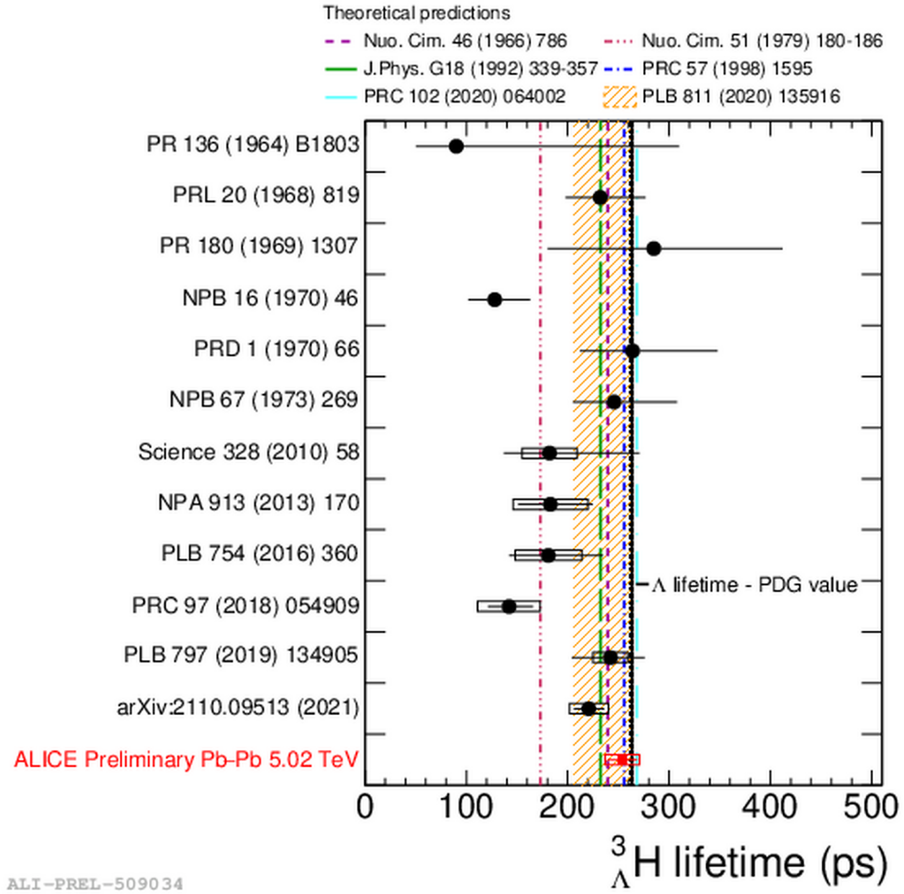

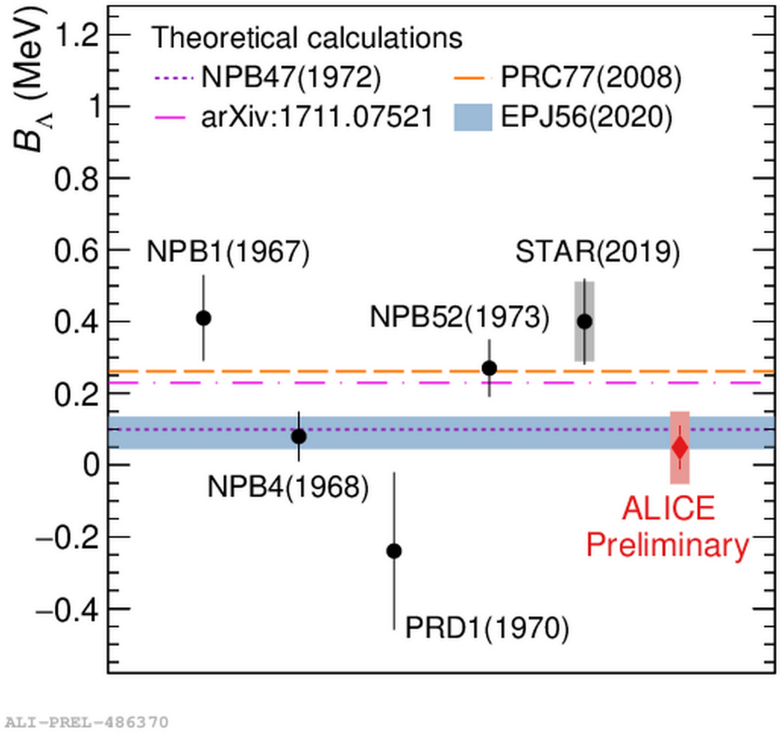

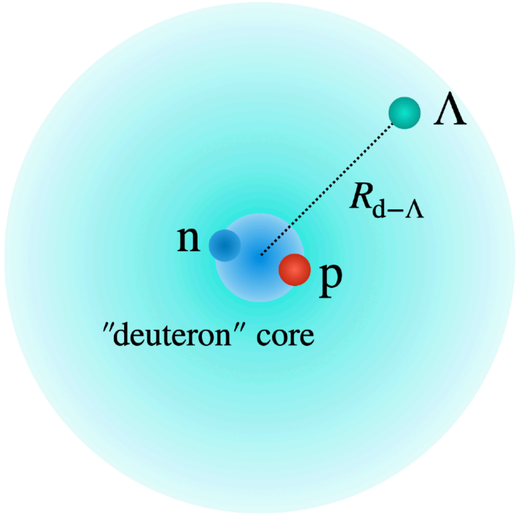

Hypertriton lifetime and Λ separation energy (B_{Λ}) measured with high precision
> consistent with weakly bound state

Λ Lifetime

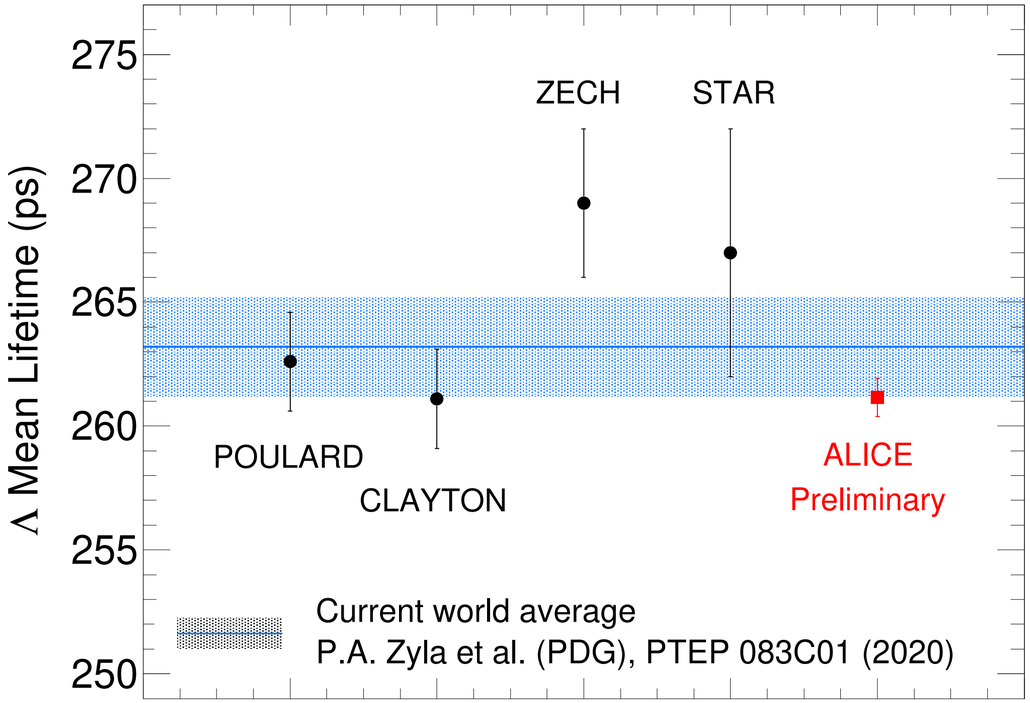

ALI-PREL-505548

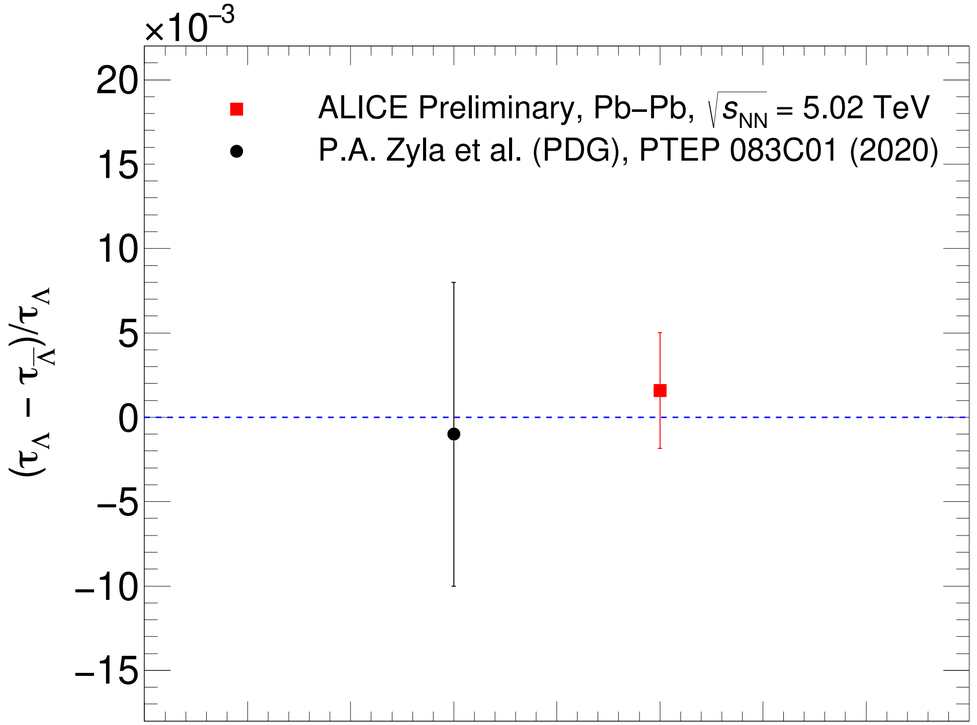

ALI-PREL-505552

Most precise measurement of the Λ and $\overline{\Lambda}$ lifetimes: almost a factor of 3 improvement wrt current world average (PDG)

$(\tau_\Lambda - \tau_{\overline{\Lambda}})/\tau_\Lambda$ consistent with zero: test of CPT symmetry in the strangeness sector

$^{3}\overline{\mathrm{He}}$ absorption

arXiv:2202.01549 [nucl-ex]

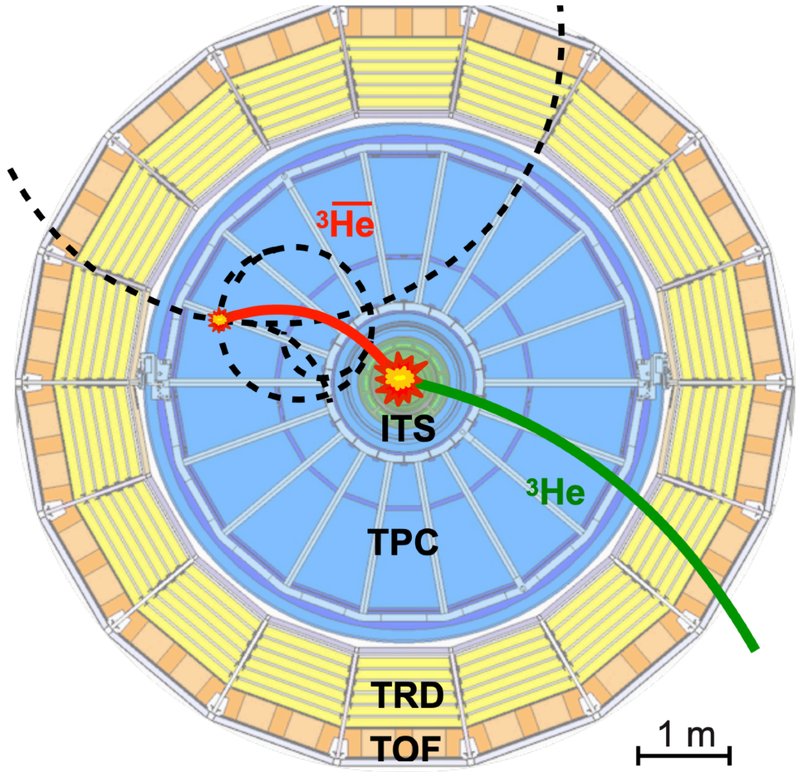

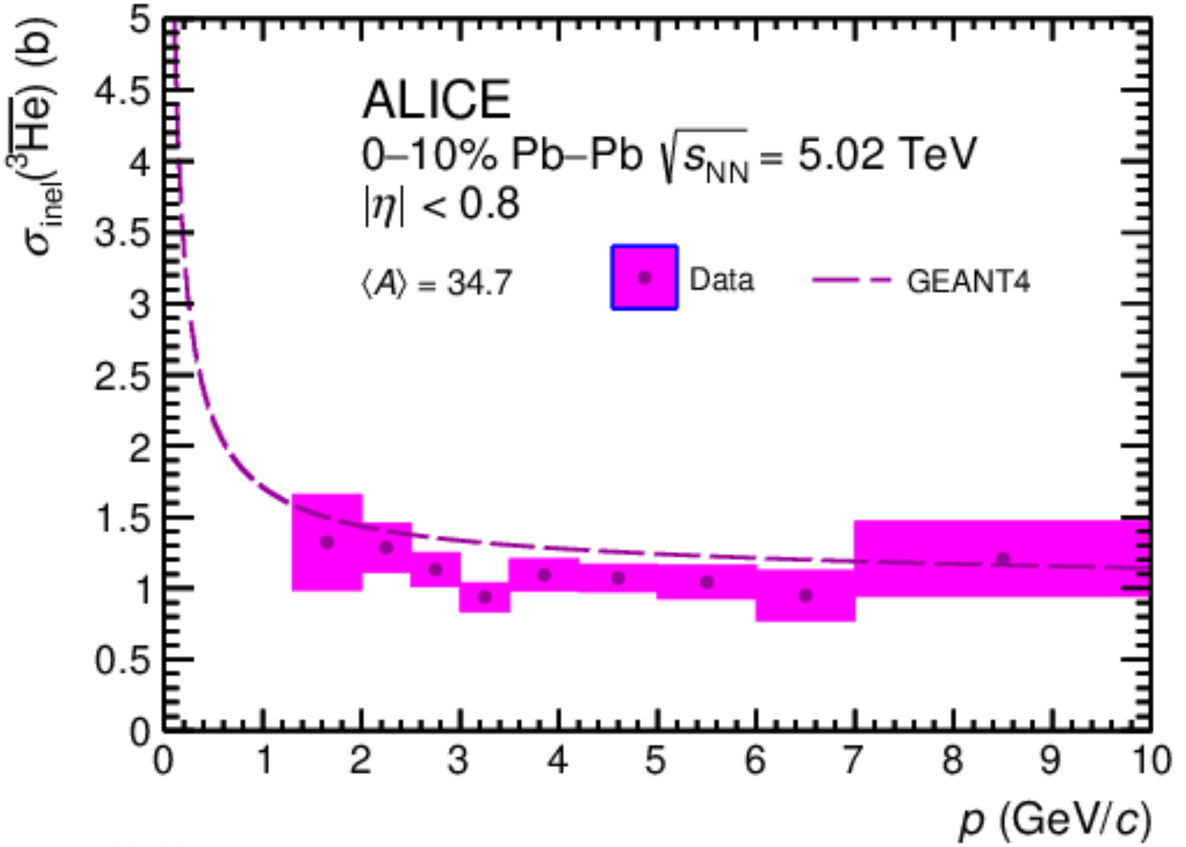

First measurement of $^{3}\overline{\mathrm{He}}$ inelastic interaction cross section with matter

~17% smaller than Geant4 (Glauber model)

$^3\overline{\mathrm{He}}$ propagation and DM searches

arXiv:2202.01549 [nucl-ex]

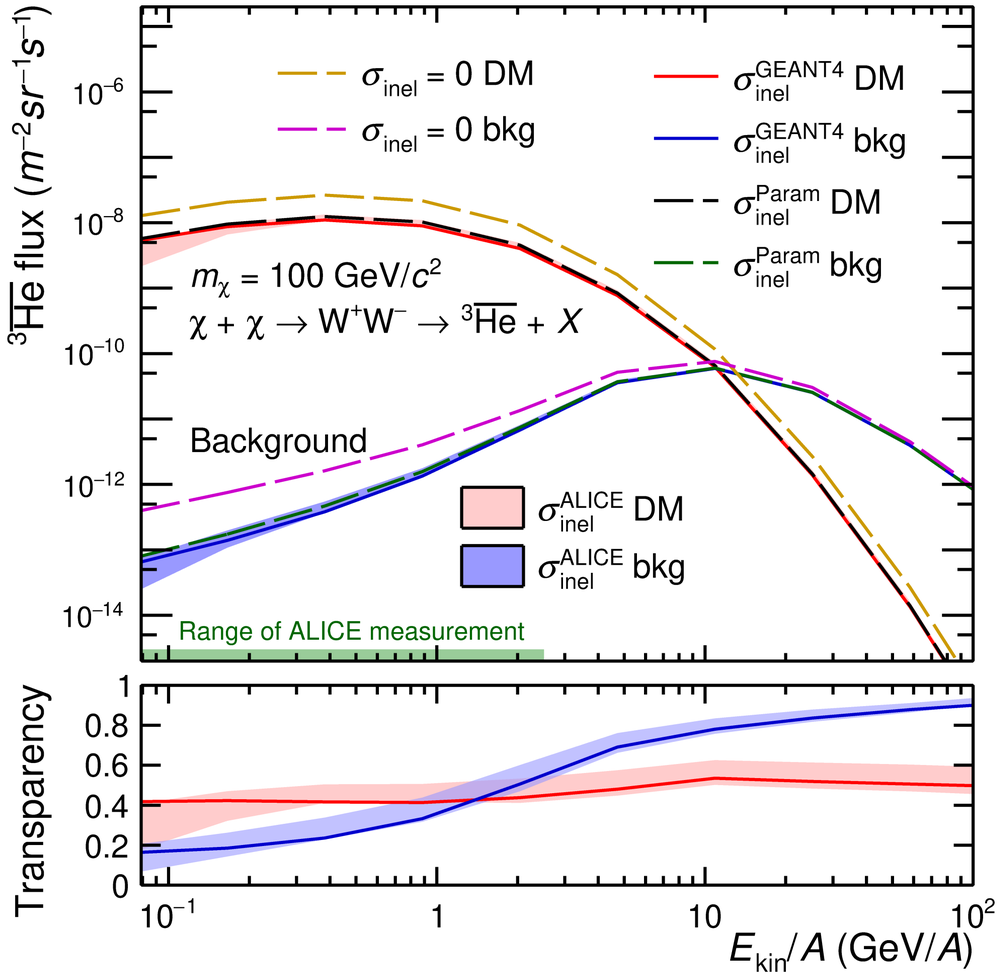

ALI-PUB-501541

$\sigma_{\mathrm{INEL}}(^3\overline{\mathrm{He}})$ used to calculate expected flux of ^{3}He from:

- Dark matter annihilation
- cosmic ray interactions with interstellar medium

Transparency of our Galaxy:

Flux using measured $\sigma_{\mathrm{INEL}}(^3\overline{\mathrm{He}})$/Flux with $\sigma_{\mathrm{INEL}}(^3\overline{\mathrm{He}}) = 0$

Strangeness and resonances

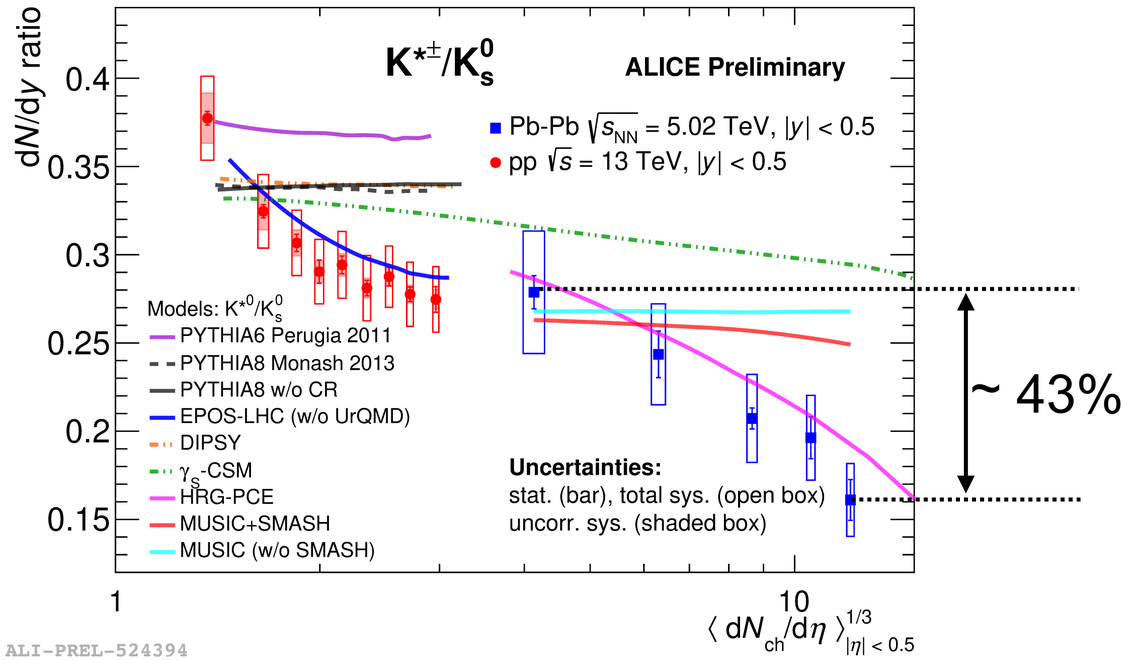

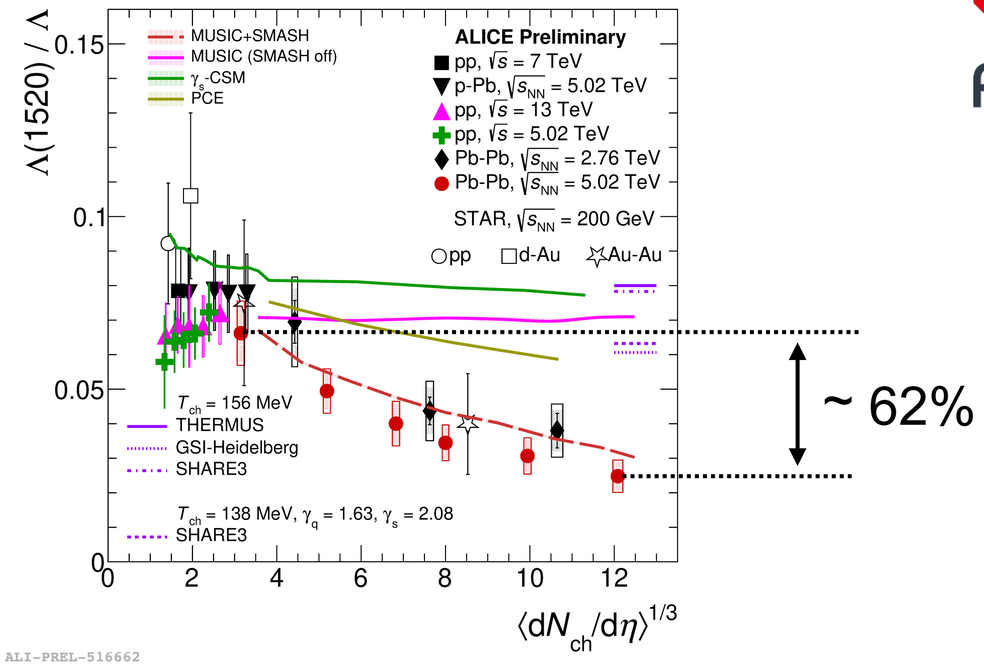

Short-lived resonances are useful tools to study hadron gas phase

$\tau_{K^*} = (4.17 \pm 0.04)$ fm/c

$\tau_{\Lambda^*} = (12.6 \pm 0.8)$ fm/c

Larger suppression for Λ^*/Λ wrt K*/K despite Λ^* has longer lifetime

> lifetime is not a good predictor (arXiv:2105.07539 **[hep-ph]**)

Data challenge existing models: Transport (SMASH) and PCE work for different resonances

Direct photons and dileptons

Direct photons

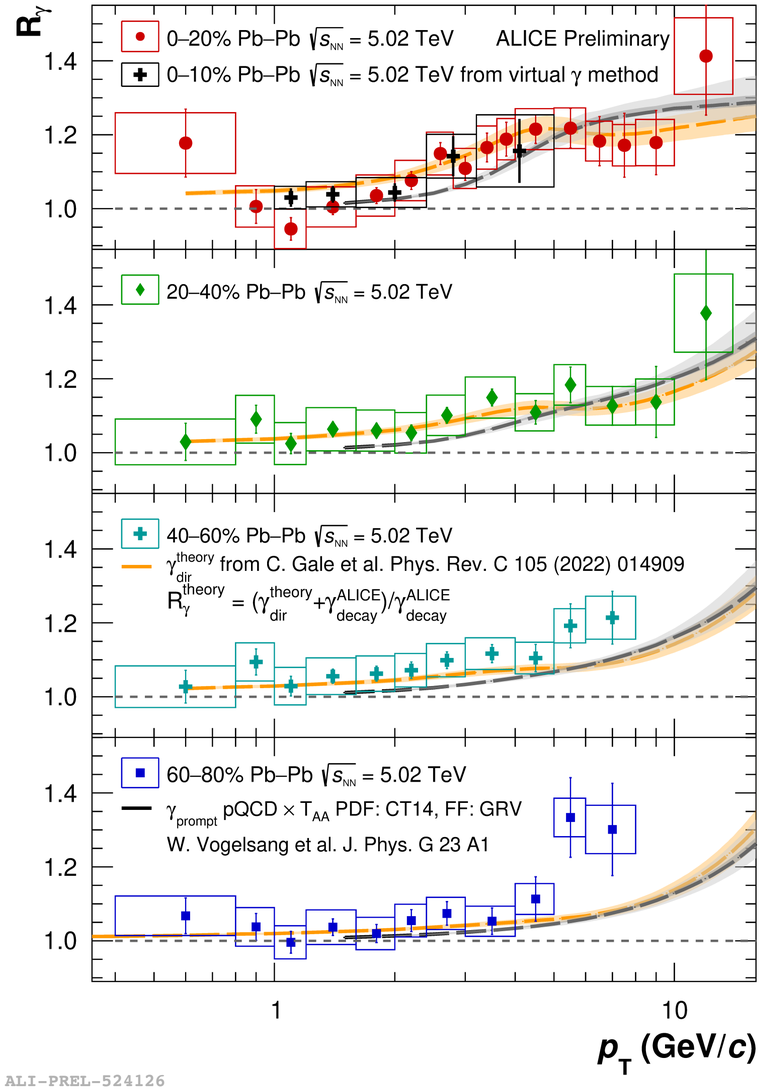

ALI-PREL-524126

$$R_\gamma = \frac{(\gamma_{dir} + \gamma_{decay})/\pi^0}{\gamma_{decay}/\pi^0_{param}}$$

Inclusive photon spectrum from data

Decay photon spectrum from simulations

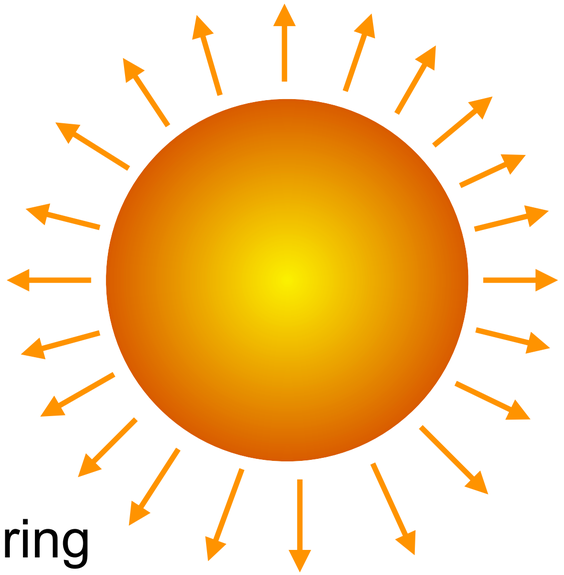

$R_\gamma > 1$ at high p_T:

- prompt photons from initial hard scattering
- can be calculated using pQCD

Hint for $R_\gamma > 1$ at low p_T:

- thermal photons from QGP
- consistent with theory calculations

Dileptons

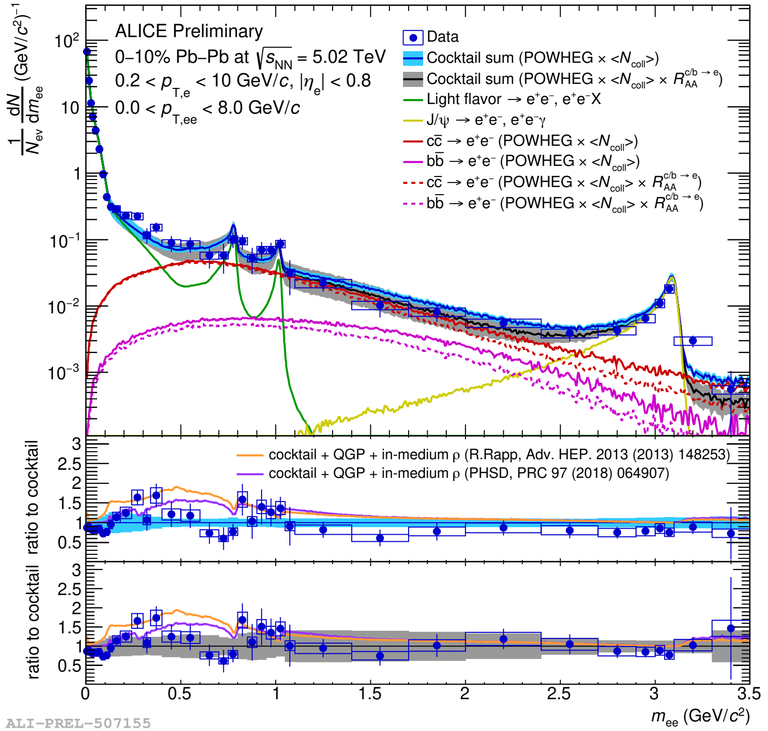

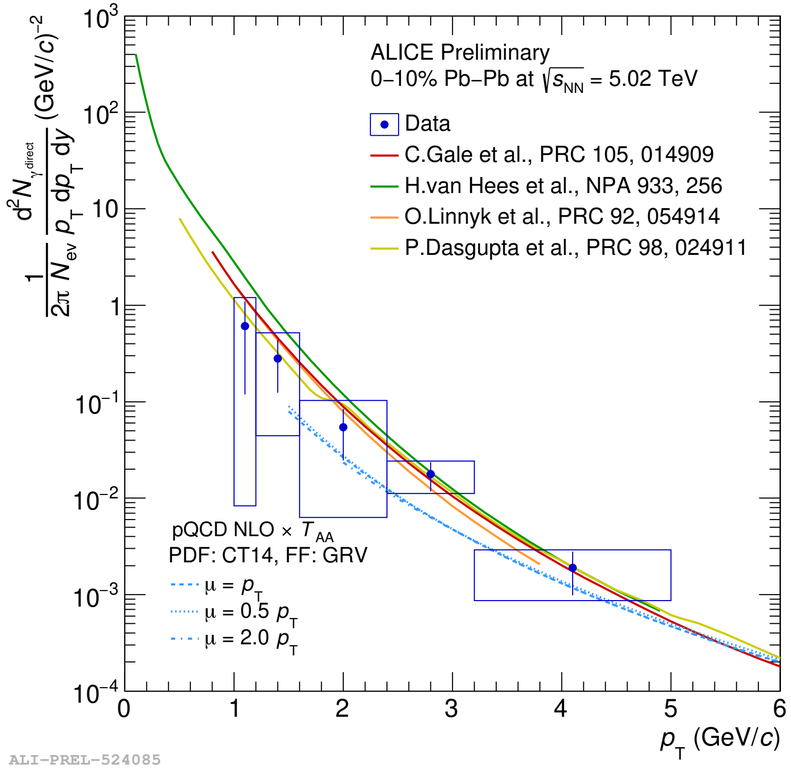

Direct photon spectrum:

$$\gamma_{dir} = \frac{\gamma^*_{dir}}{\gamma^*_{incl}} \cdot (\gamma_{incl})_{real}$$

Dilepton spectrum at LHC consistent with hadronic cocktail + QGP with in-medium ρ

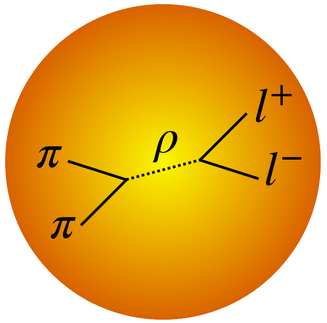

First measurement of direct γ in Pb-Pb at 5.02 TeV:

- High p_T: prompt photons consistent with pQCD
- Low p_T: data consistent with models containing in addition pre-eq. + thermal photons

ALICE upgrade

JINST 16 P03022 (2021)

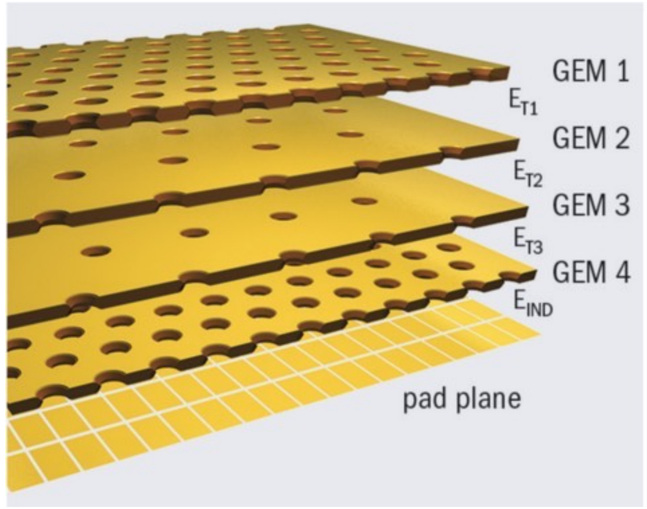

TPC upgrade:

- MWPCs replaced with GEMs
- Continuous readout @50 kHz Pb-Pb interaction rate
  > Expected increase of N_{events} by a factor 50-100 for Pb-Pb wrt Run 2
- Fully installed in August 2020

ITS Upgrade: NIM 1032, 166632 (2022)

- 7 layers of silicon pixel detectors with reduced material budget (0.35% X_0 per layer for inner barrel)
- Smaller beam pipe, 1st layer closer to interaction point (22 mm)
  > Improved pointing resolution (× 3)

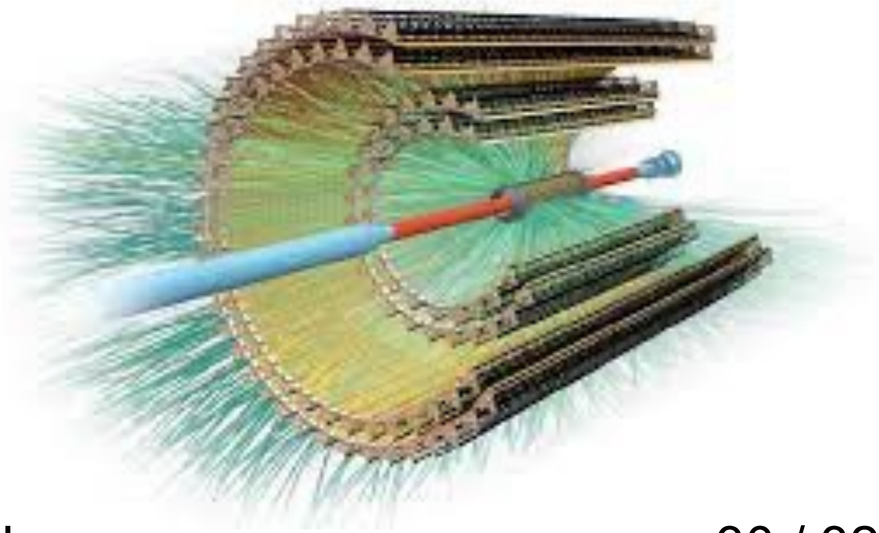

ALICE upgrade (II)

https://cds.cern.ch/record/2748310?ln=en

MFT (Muon Forward Tracker)

- high resolution Si-tracking detector installed in front of the Muon Spectrometer
- basic detection element: silicon pixel sensor (ALPIDE)
- Tracking before absorber: improve muon pointing, separation of prompt and non-prompt muons

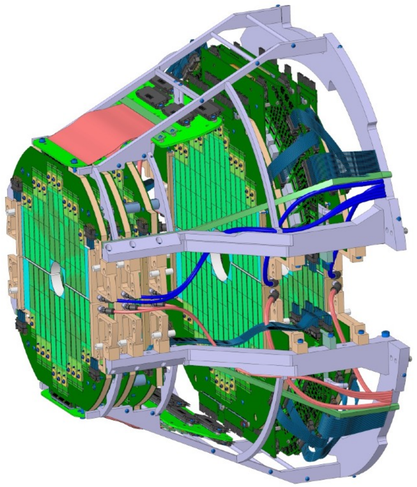

ALICE upgrade (II)

https://cds.cern.ch/record/2748310?ln=en

MFT (Muon Forward Tracker)

- high resolution Si-tracking detector installed in front of the Muon Spectrometer
- basic detection element: silicon pixel sensor (ALPIDE)
- Tracking before absorber: improve muon pointing, separation of prompt and non-prompt muons

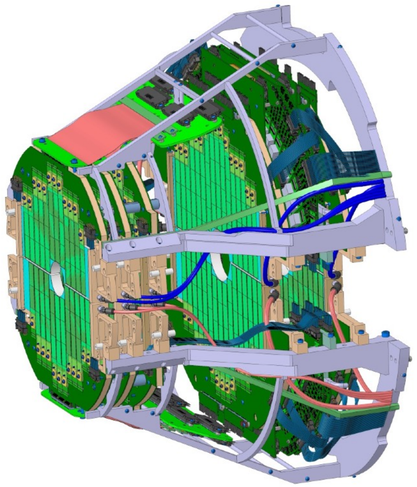

Run 3 has just started with pp collisions at 13.6 TeV

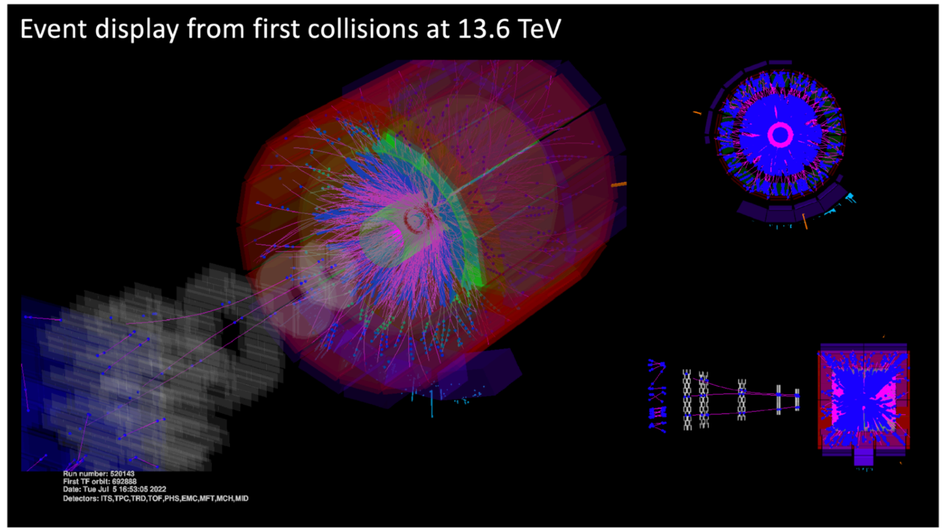

Summary

Detailed characterization of QGP properties

In-depth understanding of a large variety of phenomena have been achieved

Exciting times are ahead with the LHC Run 3

Summary

Detailed characterization of QGP properties

In-depth understanding of a large variety of phenomena have been achieved

Exciting times are ahead with the LHC Run 3

Thank you for your attention!